Development of a sample preparation method for the detection and identification of cholesterol in a Parkinson's disease model utilizing MALDI-MSI

Ingólfur Birgisson

M. Sc. thesis
University of Iceland
Faculty of Pharmaceutical Sciences
School of Health Sciences

HÁSKÓLI ÍSLANDS

Development of a sample preparation method for the detection and identification of cholesterol in a Parkinson's disease model utilizing MALDI-MSI

Ingólfur Birgisson

M. Sc. thesis in Pharmacy
Supervisor: Margrét Þorsteinsdóttir
Faculty of Pharmaceutical Sciences
School of Health Sciences, University of Iceland
May 2013

Þróun sýnameðhöndlunaraðferðar fyrir greiningu og auðkenningu kólesteróls í Parkinsons-líkani með MALDI-MSI

Ingólfur Birgisson

Meistararitgerð í lyfjafræði

Umsjónarkennari: Margrét Þorsteinsdóttir

Lyfjafræðideild

Heilbrigðisvísindasvið Háskóla Íslands

Maí 2013

Printing: Pixel ehf.
Reykjavík, Iceland 2013

Author Ingólfur Birgisson

Supervisor Margrét Þorsteinsdóttir
Associate Professor
Faculty of Pharmaceutical Sciences,
University of Iceland

Instructors Per Andrén
Associate Professor
Medical Mass Spectrometry,
Department of Pharmaceutical Biosciences,
Uppsala University

Cecilia Eriksson
Ph.D.
Medical Mass Spectrometry,
Department of Pharmaceutical Biosciences,
Uppsala University

The project was carried out at the research facilities of Medical Mass Spectrometry, Department of Pharmaceutical Biosciences, Uppsala University.

ABSTRACT

Development of a sample preparation method for the detection and identification of cholesterol in a Parkinson's disease model utilizing MALDI-MSI

Background: Findings of an association between cholesterol in the brain and Parkinson's disease (PD) have called upon further studies. The matrix-assisted laser desorption/ionization mass spectrometry imaging (MALDI-MSI) technique has been used for visualizing distribution of molecules in diseased-state tissues but has some limitations regarding analysis of cholesterol.

Objectives: 1) To develop a novel sample preparation method that facilitates analysis of cholesterol's relative abundance and distribution within the brain tissue using MALDI-MSI and enables on-tissue identification of the molecule. 2) To implement the sample preparation method in a PD-model.

Methods: Coronal brain tissue sections from control and sham-lesioned rats were used for the development of the sample preparation method. A washing preparation step with ammonium acetate buffer and a derivatization step using betaine aldehyde were evaluated both separately and combined. A unilaterally neurotoxin-lesioned PD-model rat brain was used to estimate the association between cholesterol and PD. A MALDI TOF-TOF mass spectrometer was used.

Results: The sample preparation method enables the measurements of the relative abundance and distribution of cholesterol within rat brain tissue and its identification with tandem MS (MS/MS). A combination of a washing preparation step and a derivatization step dramatically increased the signal intensity compared with no sample preparation. When performed on a PD-model no difference in relative abundance and distribution of cholesterol was observed between 6-hydroxydopamine (6-OHDA)-lesioned hemisphere and healthy tissue.

Conclusions: The sample preparation method was successful in increasing the signal intensity and allowing for an enhanced visualization of the relative abundance and distribution of cholesterol within the rat brain tissue using MALDI-MSI. Results from the PD-model suggest that cholesterol levels may not be affected in a 6-OHDA induced rat model of PD.

ÁGRIP

Þróun sýnameðhöndlunaraðferðar fyrir greiningu og auðkenningu kólesteróls í Parkinsons-líkani með MALDI-MSI

Bakgrunnur: Uppgötvuð tengsl milli kólesteróls í heila og Parkinsonsveiki hafa kallað á frekari rannsóknir. Matrix-assisted laser desorption/ionization mass spectrometry imaging (MALDI-MSI) tæknin hefur verið notuð til að skoða sameindir í sjúkum vefum en hefur ákveðnar takmarkanir þegar kemur að greiningu á kólesteróli.

Markmið: 1) Að þróa nýja aðferð fyrir sýnameðhöndlun sem auðveldar greiningu á hlutfallslegu magni og dreifingu kólesteróls í heilavef með notkun MALDI-MSI og gerir auðkenningu sameindarinnar á vef mögulega. 2) Að hagnýta aðferðina í Parkinsons-líkani.

Aðferðir: Krúnuheilasneiðar úr samanburðar og sham-löskuðum rottum voru notaðar fyrir aðferðarþróunina. Undirbúningsskref sem fólu í sér annars vegar þvott með ammóníumasetat stuðpúða og hins vegar afleiðumyndun með hjálp betaíne aldehýð voru metin bæði sitt í hvoru lagi og sameinuð. Einhliða 6-hydroxydopamine (6-OHDA)-taugaeiturs-laskaðir Parkinsons-líkan rottu heilar voru notaðir til að meta tengsl milli kólesteróls og Parkinsonsveiki. Rannsóknin var framkvæmd með MALDI TOF-TOF massagreini.

Niðurstöður: Nýja aðferðin var nýtileg til að meta hlutfallslegt magn og dreifingu kólesteróls í heilavef rottu. Samsetning þvottaskrefs og afleiðumyndunar jók merkið verulega samanborið við það að sleppa sýnameðhöndlun. Þegar aðferðin var notuð á Parkinsons-líkan sást enginn munur í hlutfallslegu magni og dreifingu kólesteróls milli vefs sprautuðum með 6-OHDA og heilbrigðs vefs.

Ályktanir: Sýnameðhöndlunaraðferðin reyndist árangursrík í að auka merkjastyrk og bæta greiningu á hlutfallslegu magni og dreifingu kólesteróls í heilavef rottu með MALDI-MSI. Enginn munur sást á hlutfallslegu magni kólesteróls í Parkinsons-módeli með hjálp aðferðarinnar, sem bendir til þess að eitrun með 6-OHDA hafi ekki áhrif á kólesterólstyrk í Parkinsons-rottumódeli.

ABBREVIATIONS

6-OHDA	6-hydroxydopamine
9-AA	9-aminoacridine
24-OHC	24 (S)-hydroxycholesterol
ABC	ATB-binding cassette
Acetyl CoA	Acetyl coenzyme A
ACN	Acetonitrile
ApoE	Apolipoprotein E
ATP	Adenosine triphosphate
BA	Betanine aldehyde
BBB	Blood-brain-barrier
CHCA	α-cyano-4-hydroxycinnamic acid
CNS	Central nervous system
CYP46A1	Cytochrome P 46A1
DA	Dopaminergic
DESI	Desorption electrospray ionization
DHB	2,5-dihydroxy benzoic acid
DMF	Dimethylformamide
EI	Electron ionization
ESI	Electrospray ionization
IP	Idiopathic parkinsonism
i.p.	Intraperitonial
ITO	Indium tin oxide
LB	Lewy bodies
LID	Laser induced dissociation
LN	Lewy neurites
MALDI	Matrix-assisted laser desorption/ionization
MALDI-MSI	Matrix-assisted laser desorption/ionization mass spectrometry imaging
MPTP	1-methyl-4-phenyl-1,2,3,6-tetrahydropyridine
MS	Mass spectrometry

MS/MS	Tandem mass
m/z	Mass-to-charge ratio
NPC	Niemann-Pick type C
PCIS	Precursor ion selector
PD	Parkinson’s disease
SIMS	Secondary ion mass spectrometry
SNpc	Substantia nigra pars compacta
TFA	Trifluoroacetic acid
TIC	Total ion current
TLC	Thin layer chromatography
TOF	Time-of-flight
UV	Ultraviolet

TABLE OF CONTENTS

LIST OF TABLES

LIST OF FIGURES

1. INTRODUCTION

Recently a connection between cholesterol and its metabolites in the central nervous system (CNS) and Parkinson's disease (PD) has been noticed (Liu et al., 2010). A relatively new mass spectrometry tool gaining a lot of interest for its qualities in visualizing the abundance and distribution of molecules within healthy or diseased tissue denoted matrix-assisted laser desorption/ionization mass spectrometry imaging (MALDI-MSI) was utilized for this assignment (Ye, Gemperline, & Li, 2012). Unpublished results from the medical mass spectrometry group located in Uppsala, Sweden revealed intriguing details on the abundance and distribution of the cholesterol molecule in a PD-tissue model, which called upon closer examination. Since cholesterol has low proton affinity and is difficult to ionize and visualize using MALDI spectrometry, an improved method needs to be developed for the consistent analysis of cholesterol with MALDI-MSI (Wu, Ifa, Manicke, & Cooks, 2009). This thesis is based on the method development aimed at being able to consistently visualize and measure the relative abundance and distribution of cholesterol and identify the molecule in rat brain tissues using MALDI-MSI.

1.1 Cholesterol

Cholesterol is an endogenous molecule, necessary for a variety of functions in the human body. It is vital in the function and structure of the cell membrane; serves as a precursor for the biosynthesis of steroids, bile acids and vitamin D; is one of the major components of lipid rafts; and participates in metabolism regulation within cells (Anchisi, Dessi, Pani, & Mandas, 2012; Liu et al., 2010; Simons & Ehehalt, 2002). Cholesterol is a sterol and is characterized by four hydroaromatic rings and a free 3-beta-hydroxy group (Figure 1) (Davis, Sinensky, & Junker, 1989; Minovici &

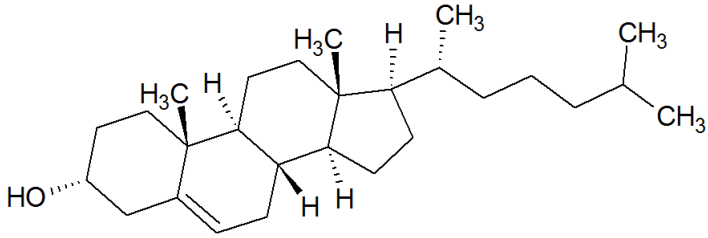

Figure 1. The structure of cholesterol.

Vanghelovici, 1934). The inclusion of cholesterol into the membrane layer of cells is facilitated by the hydroxyl group, neighboring the phospholipid heads of the polar bilayer (in contact with the aqueous surface), while the carbohydrate is surrounded by the hydrocarbon chains of the bilayer (Steck & Lange, 2010). Cholesterol is water insoluble; little exists in free solution and transportation in plasma is performed via lipoprotein particles while lipid-rich vesicles aid transportation inside the cell (Davis et al., 1989). The human brain is rich in cholesterol; while accounting for about 2% of the total bodyweight, it accommodates roughly 23% of the total body cholesterol (Dietschy & Turley, 2004; Liu et al., 2010). In spite of the high basal metabolic rate of the brain, the turnover of cholesterol is quite low (estimated as 0.03% of the cholesterol pool daily) compared to the rest of the body (0.7% of total cholesterol daily) (Dietschy & Turley, 2004).

1.1.1 Function in the CNS

The major task of cholesterol in the brain is to form myelin sheaths that cover the axons while the brain is developing. Post development, cholesterol is utilized for continued axon growth and synapse formation (Anchisi et al., 2012). Cholesterol bound to apolipoprotein E (ApoE)-containing lipoproteins from astrocytes encourages synaptogenesis in CNS neurons; when these lipoproteins derive from glia they promote axonal growth of CNS neurons (Hayashi, Campenot, Vance, & Vance, 2004; Mauch et al., 2001). In addition, cholesterol functions as a regulator of membrane signaling proteins and enzymes involved in diverse brain functions (Anchisi et al., 2012; Liu et al., 2010), and plays a role in the synthesis of neurosteroids that regulate neurotransmitter receptors (Anchisi et al., 2012).

1.1.2 Synthesis in the CNS

According to research observations, cholesterol is unable to cross the blood-brain-barrier (BBB), whether bound to apolipoproteins or in its unbound state (Dietschy, 2009; Dietschy & Turley, 2004). Unlike the rest of the body, that both synthesizes and obtains cholesterol from the diet (Ikonen, 2008), the brain synthesizes all of its cholesterol *de novo* from acetyl coenzyme A (acetyl CoA) through the mevalonate pathway (Anchisi et al., 2012).

It seems that even though neurons can produce cholesterol, the amount of cholesterol produced in the mature neuron is not enough to sustain them for continued growth of the nerve cells and so they rely on exogenously synthesized cholesterol from astrocytes (Dietschy & Turley, 2004; Nieweg, Schaller, & Pfrieger, 2009). This synthesized cholesterol is transferred from astrocytes to the neuron utilizing ApoE-containing lipoprotein particles. In the neuron this complex is taken up via receptors of the low-density lipoprotein receptor family (Dietschy & Turley, 2004; Hayashi, 2011).

1.1.3 Transportation in the CNS

Although knowledge on cholesterol homeostasis in the CNS is currently limited, a fundamental route of cholesterol transport can be proposed. After synthesis in the astrocytes, cholesterol is, in complex with ApoE, transported and excreted to the pericellular fluid by an adenosine triphosphate (ATP)-binding cassette (ABC) transporter (Dietschy, 2009). The complex moves to a neuron where it is taken up by endocytosis and transported to the late endosomal/lysosomal compartment (Aqul et al., 2011; Dietschy & Turley, 2004). The Niemann-Pick disease type C (NPC) protein delivers it to the metabolically active pool of cholesterol in the cytoplasm. In the cytoplasm, cholesterol can be esterified into storage lipid droplets, used in the membrane, or metabolized to the oxysterol 24 (S)-hydroxycholesterol (24-OHC) and moved out of the cell for elimination (Aqul et al., 2011).

1.1.4 Elimination from the CNS

Since cholesterol synthesis exceeds requirement in the adult brain, it needs to be transformed into a product able to cross the BBB. At least two pathways are believed to participate in the elimination of cholesterol (Dietschy, 2009; Dietschy & Turley, 2004; Xie, Lund, Turley, Russell, & Dietschy, 2003).

The major pathway, estimated to account for around 65% of the elimination, transforms cholesterol into 24-OHC through the neuron-specific cytochrome P 46A1 (CYP46A1) enzyme (Dietschy, 2009; Lund, Guileyardo, & Russell, 1999; Xie et al., 2003). This oxysterol crosses the BBB and is transported to the liver for excretion (Björkhem et al., 1998; Gamba et al., 2012).

The transport mechanism of the other pathway, accounting for around 35% of cholesterol elimination, is still unknown but is believed to represent the elimination from glial cells and myelin (Lutjohann et al., 1996; Xie et al., 2003).

1.1.5 Cholesterol and neurodegeneration

The cholesterol pool in the CNS is tightly regulated through the interplay of synthesis, transportation and elimination (Dietschy, 2009). A growing body of evidence suggests that a malfunction in this regulation can have adverse consequences as it has been shown that cholesterol is toxic if accumulated in the brain (Anchisi et al., 2012; Dietschy, 2009; Liu et al., 2010; Tabas, 2002).

A fault in the trafficking and levels of CNS cholesterol has been connected to neurodegenerative diseases such as Alzheimer's disease, Niemann-Pick disease C and Parkinson's disease (Anchisi et al., 2012; Liu et al., 2010). The mechanism underlying this connection between PD and cholesterol is currently undefined (Liu et al., 2010; Rantham Prabhakara et al., 2008).

1.2 Parkinson's disease

Parkinson's disease is the second most common neurodegenerative diseases in the world, affecting 1-2% of people over 65 years of age (Grünblatt, 2012; Thomas & Beal, 2011). The disease was first described in 1817 in "An Essay on the Shaking Palsy" by James Parkinson and later named after him (Jankovic, 2008; Thomas & Beal, 2007).

The disease comprises both motor and non-motor symptoms. The main motor symptoms include tremor at rest, slowness of movement (bradykinesia), poor balance (impairment of righting reflexes) and rigidity (Brooks, 2012; Jankovic, 2008; Thomas & Beal, 2011). Among non-motor symptoms are depression, cognitive impairment and sleep disorders (Jankovic, 2008).

The motor symptoms in PD result from the death of dopaminergic (DA) cells in the midbrain, especially in the ventral tier of the substantia nigra pars compacta (SNpc) (Hindle, 2010; Ozansoy & Basak, 2012). The cause of this cell death is not fully understood but includes among other things oxidative stress, failure of the ubiquitin-proteasome system, and mitochondrial dysfunction (Licker, Kövari, Hochstrasser, &

Burkhard, 2009; Samii, Nutt, & Ransom, 2004; Thomas & Beal, 2007). The pathological hallmark of PD is accumulation of the protein α-synuclein in susceptible neurons in the form of Lewy bodies (LB) and Lewy neurites (LN) (Thomas & Beal, 2007).

1.2.1 Degeneration of dopaminergic neurons

Although non-DA neurons can be affected, DA neurons seem to be specifically targeted in PD. Emphasis has been put on explaining this specific vulnerability of the DA neurons (Licker et al., 2009).

Firstly, DA neurons produce dopamine in the pre-synaptic nerve terminals, but dopamine is a very unstable molecule and can auto-oxidize, forming reactive oxygen species.

Secondly, the structure of DA neurons is unusual, with disproportionally long, thin and poorly- or un-myelinated branched axonal projections compared with a small cell body. This structure together with the use of L-type calcium channels as a means to maintain basic activity is thought to necessitate high energy production in the neurons. This makes the neurons vulnerable as it leads to high mitochondrial stress, accelerated cellular ageing and death.

Thirdly, DA neurons seem to have higher iron content than most neurons. Hydrogen peroxide that can form during dopamine auto-oxidization can react with iron and be reduced to cytotoxic hydroxyl radicals.

Lastly, levels of antioxidants are low in DA neurons, making them less able to cope with oxidative stress (Alberio & Fasano, 2011; Licker et al., 2009).

1.2.2 Risk factors

Patients displaying the classical symptoms and responding to levodopa treatment are classified as having idiopathic (or sporadic) parkinsonism (IP) (Denson & Wszolek, 1995; Jankovic, 2008). Parkinsonian patients having an identifiable cause of parkinsonism (e.g. exposure to certain toxins or drugs, brain tumors, trauma, or viral infections), deficits in the cerebellum or motor neurons, paresis of conjugate gaze, or autonomic failure, do not fit the IP classification (Denson & Wszolek, 1995).

Risk factors for the degeneration of DA neurons include ageing, genetic susceptibility and environmental exposures (Ozansoy & Basak, 2012; Samii et al., 2004).

1.2.2.1 Ageing

The largest independent risk factor associated with development of PD is higher age. Biological changes that accompany age (e.g. an increase in free radical production, mitochondrial dysfunction, oxidative stress and impairment of the brain's ability to recover from damage) are significant to the etiology and pathogenesis of PD (Hindle, 2010).

In the progress of normal ageing there is some deposition of α-synuclein and in some instances appearance of LB (Hindle, 2010; Samii et al., 2004). Some other features of ageing (e.g. decline in proteasome activity, progressive accumulation of iron in the brain, reduced efficiency of chaperones, imbalanced autophagic recycling, and complement activation) explain the higher risk of PD associated with ageing.

1.2.2.2 Genetics

For a long time PD was thought to be unconnected to genetics (Valente, Arena, Torosantucci, & Gelmetti, 2012). Now studies reveal that 10-20% of PD cases are of familial origin while the majority remains sporadic (Samii et al., 2004; Thomas & Beal, 2007). Increasing number of genes and proteins have been linked to PD, most noticeably the genes connected with the so called PARK loci (Thomas & Beal, 2007; Valente et al., 2012). Research of these genes have confirmed the genetic part of PD and also provided vital information in understanding the pathogenesis of the more common sporadic disease, as it is hypothesized that common mechanisms are at play in both the sporadic and familial form of PD (Thomas & Beal, 2007, 2011; Valente et al., 2012).

A certain pattern has been observed among autosomal dominant and recessive genes associated with PD. The genes that are autosomal dominant seem to encode for proteins that are toxic or adverse for the cells. Overexpression or mutation of these genes can lead to PD. Genes that are autosomal recessive seem on the contrary to encode proteins that have a protective effect in the brain cell (Valente et al., 2012).

1.2.2.3 Environmental factors

Environmental factors can influence PD, either adversely or protectively (Samii et al., 2004). Among risk factors are pesticides, living in rural areas, drinking well water, welding, mining and exposure of heavy metals and solvents (Hindle, 2010; Samii et al., 2004). A toxin denoted 1-methyl-4-phenyl-1,2,3,6-tetrahydropyridine (MPTP), that crosses the BBB freely and converts to MPP+ inside the astrocytes before being endocytosed by DA neurons is the only environmental agent that has been directly connected to the development of parkinsonism that is indistinguishable from PD clinically (Samii et al., 2004). Both MTPT and another neurotoxin, denoted 6-hydroxydopamine (6-OHDA), are routinely used in experiments to produce animal models designed to mimic PD (Schober, 2004).

Among factors that have been shown to have protective effects on PD are cigarette smoking, caffeine intake and use of anti-inflammatory agents (Hindle, 2010; Samii et al., 2004). Theories exist about a neuroprotective substance residing in cigarette smoke, possibly the free radical scavenger carbon monoxide. Another theory is that people at risk for developing PD are less interested in smoking (Samii et al., 2004). Theories explaining inverse relationships between intake of caffeine and/or anti-inflammatory agents and risk of developing PD are currently not well established (Hindle, 2010; Samii et al., 2004).

1.2.3 Diagnosis

Even though no cure for PD currently exists, correct and timely diagnosis is critical to limit damage and preserve quality of life by facilitating appropriate therapy aiming at slowing down disease progression and providing relief of the symptoms (Samii et al., 2004; Thomas & Beal, 2007, 2011). There are however problems regarding diagnosis.

PD is diagnosed based on the clinical features of the disease; the main motor symptoms (Jankovic, 2008). The rate of misdiagnosis is quite high, ranging from 10% by movement disorder specialists to 50% in primary healthcare (Alberio & Fasano, 2011). Current knowledge suggests that the appearance of clinical symptoms occur after 70-80% of the striatal dopamine has been lost and about 50-70% of the neurons have been destroyed; thus the clinical diagnosis occurs in advanced stages of neurodegeneration (Haas, Stewart, & Zhang, 2012; Muller, 2012; Ozansoy & Basak,

2012). Additionally, a definite diagnosis can only be made during autopsy with the inspection of the pathological hallmark of PD; accumulation of the protein α-synuclein in susceptible neurons in the form of LB and LN (Haas et al., 2012; Jankovic, 2008). It is not fully known whether LB and LN form as a response to the accumulation of α-synuclein providing a protective mechanism or are a part of the pathogenesis of PD. Results from studies incline towards them being protective (Thomas & Beal, 2007).

1.3 Cholesterol levels in the CNS and Parkinson's disease

Certain connections have been established between PD and the cholesterol molecule within the brain. A certain allele of the gene encoding for ApoE, the main cholesterol transporter within the brain has been linked with a higher risk and earlier onset of PD (Mahley, Weisgraber, & Huang, 2006). The oxysterol metabolites of cholesterol have been found to interact with certain enzymes and factors connected to PD pathology, such as generation of free radicals and influence on α-synuclein accumulation (Rantham Prabhakara et al., 2008). The metabolites of cholesterol have also been shown to be increased in DA neurons in a degenerative state with elevated α-synuclein deposition (Bar-On et al., 2008; Bosco et al., 2006).

Like mentioned before, one of the cardinal hallmarks of PD is α-synuclein accumulation and interaction of this protein with cholesterol has been noted (Liu et al., 2010). An indicator of a connection between the two molecules is that the concentration of cholesterol is increased in mice model lacking α-synuclein. This could be due to the proposed role of α-synuclein in the transfer of cholesterol and the interaction of α-synuclein with lipid rafts and vesicle membranes, of which cholesterol is a major component. It is also intriguing to note that in α-synuclein aggregation, which happens in PD pathogenesis, is associated with cholesterol among other lipids (Bar-On et al., 2008; Barceló-Coblijn, Golovko, Weinhofer, Berger, & Murphy, 2007; Fortin et al., 2004; Kamp & Beyer, 2006; Liu et al., 2010).

A relatively new method, MALDI-MSI has the power to visualize the distribution of molecules and compare the composition between healthy and diseased tissue. This method has been praised for its application in examining diseased tissue and

obtaining information on molecular pathology of various diseases, for example neurodegenerative diseases (Ye et al., 2012).

1.4 MALDI

Matrix assisted laser desorption/ionization (MALDI) mass spectrometry imaging (MSI) emerged in 1997, 10 years after the original invention of MALDI (Caprioli, Farmer, & Gile, 1997). Although this technique is relatively new it has been utilized successfully in localization of proteins, distribution of lipids, pharmacology, and identification of biomarkers from tissue sections (Heeren, Smith, Stauber, Kükrer-Kaletas, & MacAleese, 2009; Ye et al., 2012). This is due to the fact that this method directly ionizes and detects molecules present in a tissue segment (Goto-Inoue, Hayasaka, Zaima, & Setou, 2011).

MALDI-MSI has particularly found its niche as a biomarker discovery tool since it does not require any target specific handling before the application (Schwamborn, 2012; Schwamborn & Caprioli, 2010; Ye et al., 2012). As such it has been used to aid in the diagnosis of disease or to assess the response of subjects to drugs (Ye et al., 2012).

1.4.1 MALDI methodology

The MSI group comprises different methodologies along with MALDI (Ye et al., 2012). The methods differ mainly in the ionization technique and sometimes in the handling of tissue. Other techniques besides MALDI that are mainly used for acquiring MSI data from tissue are desorption electrospray ionization (DESI) and secondary ion mass spectrometry (SIMS) (Chaurand, 2012; Ye et al., 2012).

1.4.1.1 Ionization

MALDI is a soft ionization method that applies a pulsed ultraviolet (UV) laser to desorb and ionize molecules that have been mixed with a matrix (Chaurand, 2012). The matrix is usually a small organic substance that has the ability to absorb energy at the wavelength that the laser emits and thus facilitates analyte ionization (Goto-Inoue et al., 2011; Touboul, Brunelle, & Laprévote, 2011). In the case of MALDI-MSI the matrix is deposited on the segmented tissue before ionizing and crystallizes upon drying

(Chaurand, 2012; Goto-Inoue et al., 2011; Schwamborn & Caprioli, 2010). The method commonly produces singly charged ions, which facilitates analysis and data processing (Cameron, 2012; Ye et al., 2012). The lasers commonly used in MALDI are nitrogen or neodymium-doped yttrium aluminum garnet lasers that work at a fixed wavelength (Touboul et al., 2011).

MALDI has the ability to ionize biomolecules varying in size from mass-to-charge ratios (m/z) as small as <1000 Da to the considerable size of >100 kDa. This feature allows it to be utilized in diverse fields such as lipidomics, proteomics and analysis of small molecules (Chaurand, 2012; Goto-Inoue et al., 2011).

1.4.1.2 Instrumentation

The MALDI ionization source is commonly coupled with a time-of-flight (TOF) analyzer (Chaurand, 2012; Goto-Inoue et al., 2011; Touboul et al., 2011). In those analyzers, the m/z of the ions is determined by the time it takes them to fly through the TOF tube after acceleration to the same kinetic energy (Ye et al., 2012). After receiving the same energy in a charged grid the ions drift freely through the tube where mass separation is achieved (Fuchs, Süß, & Schiller, 2010). Since the same kinetic energy is achieved, the time it takes the ions to reach the detector depends directly on their m/z. This results in smaller ions reaching the detector sooner than larger ions, and so m/z can be calculated (Touboul et al., 2011).

The major advantages of TOF analyzers are high mass sensitivity and mass accuracy along with a wide mass range (Murphy, Hankin, & Barkley, 2008; Ye et al., 2012). They perform at a highly rapid mass obtaining speed and exhibit no loss of ions as all ions generated by the MALDI ionization are collected (Murphy et al., 2008). One of the reason TOF analyzers are popularly combined with MALDI ion source is that the pulsed, not continuous, ion generation of the MALDI source is most applicable with the TOF analyzer (Fuchs et al., 2010).

The major drawback of the TOF analyzers is the low mass resolving power it possesses (Jungmann & Heeren, 2012). In order to improve the mass resolution tandem TOF analyzers have been made and reflectron grids have been added to lengthen the travelling distance (Fuchs et al., 2010; Touboul et al., 2011). The addition of tandem mass spectrometry (MS) techniques to the TOF analyzers allows for MS/MS

fragmentation and more accurate identification (Goto-Inoue et al., 2011; Touboul et al., 2011; Ye et al., 2012).

1.4.1.3 MALDI-MSI

In MALDI-MSI, the laser or ion beam is focused on a spot where a single mass spectrum is obtained. The laser beam then moves over the tissue in preset order, gathering mass spectra at each X,Y coordinate (Heeren et al., 2009; Murphy et al., 2008). This information is then transferred into a database containing four dimensional information, the X,Y-coordinates, m/z and ion abundance. This data is used with an optical image of the tissue section to compile an image which conveys distribution and abundances of the ionized molecules (Murphy et al., 2008).

A very important process for correct interpretation of the information produced from MALDI-MSI experiments is normalization. This is vital for removing artifacts that can affect the mass spectral intensity of all or only a selection of signals in the MALDI spectra. The artifacts can be a product of a variety of factors such as; matrix crystal distribution; ion source contamination which causes fading of signal along the path of spectra acquisition; variance in chemical objects such as pH gradient, salt distribution and phospholipid background structure (Deininger et al., 2011). The standard normalization process is based on the total ion current (TIC) where each spectrum is divided by the square root of the sum of the squared intensities (Duncan, Roder, & Hunsucker, 2008). This normalization method is most often beneficial but in certain cases it can produce misleading results. This is particularly a hazard where the signal of prominent abundance is confined to small areas (Deininger et al., 2011).

The main advantage of MALDI-MSI is that pre-selection of analyte in the sample is not needed to detect the molecule of choice (Goodwin, 2012). Other imaging techniques need to use radioactive or fluorescence labeling prior to visualization, making the pre-selection of analyte necessary. MALDI-MSI circumvents this need of pre-selection and modification of molecules as the compound's molecular mass is utilized as an endogenous label (Heeren et al., 2009; Jungmann & Heeren, 2012). Another quality of MALDI-MSI is that it is relatively easy to operate (Goodwin, 2012).

Quantitation of analytes has been the Achilles heel of MALDI-MSI but efforts are being made to rectify this disadvantage (Duncan et al., 2008; Ye et al., 2012), for

example by developing a software for reproducible quantitation with the assistance of labeled standards for MALDI-MSI (Källback, Shariatgorji, Nilsson, & Andrén, 2012). Compound identification has been described as a bottleneck for the imaging MS methods but this refers more to identifications of proteins and less to lower molecular weight molecules such as metabolites and lipids (Chaurand, 2012). Another disadvantage of MALDI-MSI is that it requires vacuum. This limits its application to live biological samples, for instance in the clinical setting (Ye et al., 2012). This could however change as MALDI-MSI in atmospheric pressure has been successfully performed for the analysis of plant and fruit tissue (Li, Shrestha, & Vertes, 2006, 2007).

1.4.2 Tissue sample preparation for MALDI-MSI

Some general procedures are done on the sample tissue segment before it is ready for analysis by the MALDI-MSI machine. This process can be roughly divided into 5 stages: collection of the tissue, storage, sectioning, post-sectioning processing and then matrix application (Goodwin, 2012).

1.4.2.1 Collection

After the animal has been euthanized according to the local guidelines the organ tissues of choice should be removed rapidly and stabilized to prevent delocalization and degradation of tissue molecules. The method of euthanasia can have more effects on certain organs than others (Goodwin, 2012). The tissue is normally flash frozen in isopentane, liquid nitrogen or alternatively frozen on dry ice (Chaurand, 2012).

1.4.2.2 Storage

After snap-freezing the tissue it should be directly transported to a freezer and kept at -80°C or lower to preserve the spatial organization of molecules and minimize degradation and other processes in the tissue (Chaurand, 2012; Goodwin, 2012; Goto-Inoue et al., 2011). The tissue should only be removed from the freezer upon use and returned as soon as possible. Transportation should be performed with the tissue on dry-ice (Goodwin, 2012; Ye et al., 2012). Whole tissues can be stored for up to a year at -80°C without any unfavorable degradation being reported (Goodwin, 2012).

1.4.2.3 Sectioning

The format in which the tissue is normally analyzed is through thin sections (Ye et al., 2012). These sections are cut in a cryostat microtome and animal tissues are usually cut to 10-20 μm thick sections (Goodwin, 2012). Thinner sections have been recommended for the analysis of high molecular weight molecules of about 3-21 kDa. The thickness of the sections can have an impact on the analysis as it affects the ionization effectiveness (Goto-Inoue et al., 2011). The temperature inside the cryostat microtome chamber usually ranges from -16 to -26°C where more dense tissues can withstand higher temperatures (Goodwin, 2012). After cutting the segment it is then traditionally thaw-mounted on conductive indium tin oxide (ITO)-coated glass slides that can be analyzed by MALDI-MSI, although adhesive film has also been used (Goto-Inoue et al., 2011). Thaw-mounting refers to the transferral and fastening of the frozen tissue on to the ITO-glass by gently touching it with a warm surface (Goodwin, 2012).

1.4.2.4 Post-section processing

After removing the tissue from the freezer after sectioning, the first step is to dry the tissue. The use of a desiccator, freeze drying, dehydration by solvent washing, and air drying with the use of nitrogen are all commonly used drying methods. Different processes exist that either aim at removing unwanted substances from the tissue or adding substances to modify the sample. Both are performed to enhance the ionization of the target species and thus sensitivity. Processes also exist to aid quantification of the sample (Goodwin, 2012).

One of the more routinely used technique is washing of the tissue. This can be performed either to remove ions that suppress the signal of the analyte of choice or to remove other molecules such as lipids for proteomic MSI or other things that can interfere with the signal from the preferred molecules. The washing process is performed carefully with the target analyte in mind so that the molecules intended for analysis are not accidentally removed (Chaurand, 2012; Goodwin, 2012).

Smaller molecules can be hard to detect, either because they are not easily ionized or because endogenous compounds with similar mass disturb the signal from the target molecule. Sample derivatizations using chemical reactions, either adding to the ionization or moving the signal peak of the target molecule to a range where other

molecules do not disturb the signal have been performed, thereby increasing detection of the small target molecules (Goodwin, 2012).

After the stabilization of samples, optical images will have to be taken to compare between the optical image and the MSI data acquired. Before taking the optical image, markers should be added onto the slide which allow for triangulation between the optical image and the MALDI-MSI machine so that the mass spectrometer can determine the required ionization positions. Flat-bed scanners and digital cameras mounted onto a micro lens have been utilized for the purpose of acquiring optical images (Goodwin, 2012).

1.4.2.5 Matrix application

The choice of a matrix compound and its homogenous application is one of the most critical preparation steps for MALDI-MSI analysis (Goto-Inoue et al., 2011; Ye et al., 2012). Among commonly used matrices are 2,5-dihydroxy benzoic acid (DHB), α-cyano-4-hydroxycinnamic acid (CHCA) and 9-aminoacridine (9-AA) (Goodwin, 2012; Ye et al., 2012). Matrices are usually organic acids that have the ability to absorb the wavelength that the laser emits (Chaurand, 2012). The mechanism of the matrix-analyte co-crystals is that when the laser hits the co-crystals the majority of the energy is absorbed by the matrix. This is due to the fact that the matrix is present in a major excess over the analyte, usually 100-100,000-fold excess. The absorption of energy causes the matrix to be vaporized, transferring the intact analyte into the vapor phase. In this vapor phase ions, for instance H^+ and Na^+, exchange between the matrix and analyte which leads to charging of the analyte. The products of analyte charging are called adducts or quasimolecular adducts (Fuchs et al., 2010). For this mechanism to happen efficiently, the application of the matrix must be uniform and the matrix-analyte crystals should be smaller than the tissue features being analyzed (Heeren et al., 2009). The application must not promote significant migration or delocalization of the target analyte (Chaurand, 2012).

The most common matrix application methods are spraying, spotting, sublimation and dry application (Chaurand, 2012; Goto-Inoue et al., 2011).

Spraying the matrix is the most commonly used method for matrix coating the sample. This method utilizes equipment such as thin layer chromatography (TLC)-

sprayers and artistic airbrushes as well as automated sprayers like the TM-sprayer from HTX imaging and the ImagePrep device from Bruker Daltonics (Goto-Inoue et al., 2011). The spray methods have the advantages of good control of matrix deposition and thickness. The manual spraying apparatus have the quality of rapid coating of the tissue but the automated sprayers offer better regulation of spraying conditions including temperature, deposition pattern and often thickness. The dimensions of the matrix crystals that form using spray method coating are ≥20 μm limiting the spatial resolution for MALDI-MSI only by the diameter of the laser beam on target (Chaurand, 2012).

The method of spotting the matrix on the tissue to be analyzed utilizes automatic deposition devices that can print microdroplet arrays on the tissue sections. This leads to the formation of high crystal density microspots that have less than 200 μm dimensions. The advantages of this method are minimal delocalization of the analyte (because the spots do not touch), high reproducibility and good signal quality. The downside of this method is lower spatial resolution (Chaurand, 2012; Goto-Inoue et al., 2011).

The sublimation of matrix on tissue is a newer method for matrix application that does not utilize any solvent (Chaurand, 2012; Goto-Inoue et al., 2011). The product is a sample with very uniform coating of matrix, increasing the analyte signal and yielding fine microcrystals, thus decreasing the limitation of image resolution caused by matrix application (Goto-Inoue et al., 2011). However the sensitivity has been questioned and is thought to be decreased because of less matrix-analyte interaction (Ye et al., 2012).

Dry-coating of the tissue sample by the use of a fine sieve to deposit the matrix does not produce a completely uniform layer of matrix. However, the imaging can be performed with high spatial resolution but suffers from the same shortcoming as sublimation; lower sensitivity (Chaurand, 2012; Ye et al., 2012).

1.4.3 Lipidomics and MALDI-MSI

Lipidomics has been defined as: “the full characterization of lipid molecular species and of their biological roles with respect to expression of proteins involved in lipid metabolism and function, including gene regulation” (Fuchs et al., 2010). This is a complex task but the first steps is to gather insights on the qualitative and quantitative lipid composition of a sample (Fuchs et al., 2010).

Lipids are organic compounds that are usually insoluble in water but soluble in organic solvents such as chloroform and methanol. They make up a big fraction of the organic molecules in a cell (Murphy et al., 2008; Touboul et al., 2011). The lipid group comprises eight categories: glycerolipids, glycerophospholipids, sphingolipids, saccharolipids, polyketides, sterol lipids, prenol lipids and fatty acyls (Touboul et al., 2011). Lipids are very diverse in chemical structure as well as their function (Murphy et al., 2008). The composition and distribution of lipids in a given cell is dynamic and deviates between different cell types and cells at different physiological conditions (Murphy et al., 2008; Touboul et al., 2011). The knowledge on distribution of specific lipid classes within tissues and the distribution of individual lipid species within cells and tissue compartments is very limited. This lack of knowledge partly stems from the absence of analytical methods that have the power to localize specific lipids without causing changes to their structure (Murphy et al., 2008).

The analytical methods traditionally used for lipid identification and quantification are gas or liquid chromatography coupled to a mass spectrometer. The downfall with these methods is that the extraction and purification steps lead to loss of lipid distribution on the tissue. Chemical imaging techniques utilizing staining or antibodies have been performed for lipid observation. The setback with these methods compared with MSI is that they target either the total lipid fraction or only one family. MSI on the other hand gives information about the whole lipid fraction, both the localization and its composition, in a single experiment (Goto-Inoue et al., 2011; Touboul et al., 2011).

Of the MSI techniques available, MALDI-MSI is the most commonly used, and by some considered the best available, method for lipid imaging (Goto-Inoue et al., 2011). For lipidomics and small molecules DHB and CHCA are the most commonly used matrices and are thought to be the most suitable (Goodwin, 2012; Goto-Inoue et al., 2011; Touboul et al., 2011).

1.4.3.1 Cholesterol and MALDI-MSI

Cholesterol is classified as a sterol lipid (Chang, Chang, Ohgami, & Yamauchi, 2006). It has very low proton affinity and low acidity and for that reason it is less well suited for analysis by MALDI and electrospray ionization (ESI) ion sources than for example

electron ionization (EI) (Johnson, Brink, & Jakobs, 2001; Tian, Failla, Bohn, & Schwartz, 2006). MALDI-MSI has difficulty detecting molecules that are not easily ionized as numerous molecules will be competing for ionization. The molecules that ionize more easily preferentially reach the detector suppressing the ionization of other molecules (Goto-Inoue et al., 2011). The relatively small mass of cholesterol can also be problematic as the matrix background can have an overlapping spectrum with the m/z peak of cholesterol (Fuchs et al., 2010). It is worth noting that when analyzed in the MALDI ion source, cholesterol is not detected as the $[M+H]^+$ peak like most molecules but rather with the elimination of water peak $[M+H^+-H_2O]$ (Fuchs et al., 2010; Murphy et al., 2008; Schiller et al., 2004). Therefore the cholesterol mass spectrometry peak is at 369.3 m/z rather than 387.3 (Schiller et al., 2004). When tandem MS is used with 369.3 as the parent ion, the major fragments appear at m/z 161, 147, 109 and 95 according to literature (Piehowski et al., 2008).

Washing is a sample preparation step that has recently been utilized both for the increase of signal intensity of lipids (cholesterol not examined) (Angel, Spraggins, Baldwin, & Caprioli, 2012) and for the improved signal intensity of small molecular substances (Shariatgorji et al., 2012).

This difficulty in ionization of cholesterol with MALDI and other ion sources, such as ESI has driven the use of methods to achieve increased cholesterol sensitivity. One of the sample preparation methods often used for enhancing the signal intensity of cholesterol is the use of a reactant to derivatize cholesterol into a product more suitable for analysis (Johnson et al., 2001; Liebisch et al., 2006; Sandhoff, Brügger, Jeckel, Lehmann, & Wieland, 1999). In these methods the reaction takes place in a solution containing cholesterol and the reactant, which implies that the reaction might not occur rapidly. This kind of derivatization method is not suitable for on-tissue MALDI-MSI sample preparation as delocalization of molecules might happen (Goodwin, 2012). The DESI MSI technology resolved this issue by using the reactant betaine aldehyde (BA) for on tissue derivatization of cholesterol (Wu et al., 2009). BA reacts fast and selectively with alcohols by nucleophilic addition, creating a charged hemiacetal salt (Figure 2) (Wu et al., 2009).

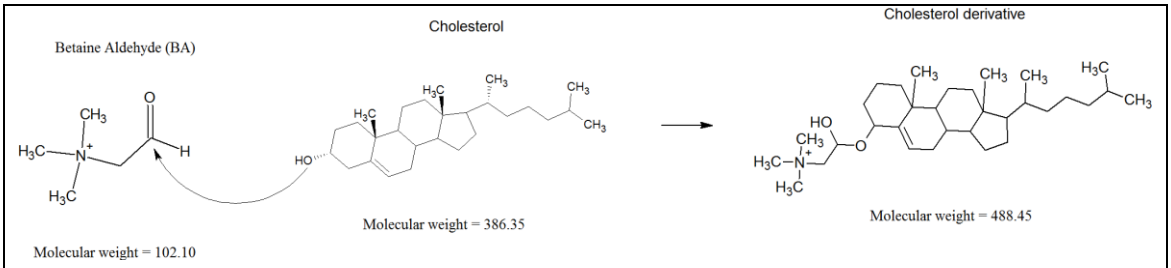

Figure 2. The reaction of betaine aldehyde with cholesterol to form the cholesterol derivative.

This tags the target molecule with a positive charge facilitating ionization and additionally moving the molecule in the mass spectra to the m/z value of (M+102.1), where M is the molecular weight of the molecule targeted and 102 is the molecular weight of BA. This transfers the cholesterol peak from m/z 369.35 to m/z 488.45. Because of the ability of BA to react with alcohol groups, care must be taken to choose the solvent system correctly to circumvent reacting the substance before applying it to the tissue. As an example methanol, that reacts very efficiently with BA, should be excluded in the solvent. Water also reacts with BA but much less efficiently, therefore some of the reactant is likely to survive until tissue application. When tandem MS is performed with m/z 488, the new derivative peak, as the parent ion the same major peaks are noticed as when 369 is the parent ion except three new peaks are added, m/z 102, 120 and 369 belonging to [BA^+], [$BA+H_2O^+$] and the cholesterol elimination of water peak, respectively. BA is believed to be especially useful for molecules containing only one hydroxyl group and with low proton affinity which matches the description of cholesterol perfectly (Wu et al., 2009).

The 6-OHDA rat animal model used in this project is designed to mimic PD as 6-OHDA is a neurotoxin that degenerates DA neurons and depletes the striatal dopaminergic levels (Schober, 2004).

There are certain structures within the brain that are likely to show high amounts of relative abundance of cholesterol. Because myelin sheaths are thought to contain 80% of cholesterol, white matter structures, where myelin sheaths are dominant, would be presumed to show the highest relative abundance of cholesterol with MALDI-MSI. Examples of such structures are the corpus callosum and a certain part of the striatum (Dietschy & Turley, 2004; Trim et al., 2008; Veloso et al., 2011).

2. OBJECTIVES

2.1 Primary objectives

To develop a sample preparation method that facilitates analysis of cholesterol's relative abundance and distribution within the brain tissue using MALDI-MSI and enables on-tissue identification of the molecule.

To implement the sample preparation method for the analysis of a Parkinson's disease animal model.

2.2 Secondary objectives

To test a sample washing preparation step for MALDI-MSI.

To test a sample derivatization preparation step for MALDI-MSI.

To compare different matrix application strategies for MALDI-MSI.

To test the combined sample preparation method which includes the sample preparation steps of washing, derivatization and matrix application.

3. MATERIALS, INSTRUMENTS AND METHODS

3.1 Materials

Table 1. Materials, manufacturer and catalogue or batch number

Material	Manufacturer	Catalogue # or Batch #
Derivatization		
Betaine aldehyde chloride	Sigma-Aldrich	B3650
N,N-Dimethylformamide	Sigma-Aldrich	99196EJ
Matrix application		
Acetonitrile	Merck	I659830242
Chloroform	Merck	K42512645131
Cholesterol min 99%	Sigma-Aldrich	362794
2,5-Dihydroxybenzoic acid	Merck	S6313645
Ethanol	Solveco	6087286
LiChrosolv water	Merck	Z285833304
Methanol	Merck	I672807306
Trifluoroacetic acid	Sigma-Aldrich	T6508
Washing preparation		
Ammonium Acetate	Fluka	09690

3.2 Instruments and equipment

Table 2. Instruments and equipment

Instrument/Equipment	Manufacturer	Version/Series
Tissue preparation		
Analogue Multimeter	Caltech	AG1100
Cryostatmicrotome	Leica	CM1900UV
Desiccator	Bel art	Space saver
Freezer (-80°C)	Labassco	Sanyo
Glass slides, ITO covered	Bruker	Glass slides for MALDI imaging
Glassware	Duran	-
Pipettes	Mettler Toledo	Volumate
Pipette tips	Gilson	Diamond
Derivatization		
Automated vaporizer	Bruker	ImagePrep
Eppendorf vials	Eppendorf	Safe-lock tubes 1.5 mL
Freezer (-18°C)	Electrolux	Eul3109
Refrigerator	Husqvarna	Opal
Matrix application		
Automated sprayer	HTX-Imaging	TM-sprayer
Conical tubes	BD Falcon	15 mL
Manual sprayer	Kontes	TLC sprayer
Scale	Mettler Toledo	35100008
Vortex	Labora	Vortex-Genie 2
MALDI-MSI analysis		
MALDI-TOF-TOF analyzer	Bruker	Ultraflextreme
Software		
Fleximaging	Bruker	Version 3.1
Isotopepattern	Bruker	Version 2.0

3.3 Methods

3.3.1 Tissue preparation

Rat brains were obtained from Karolinska Institutet in Stockholm. Male Sprague–Dawley rats (150 g; Scanbur, Sweden) were used for this study and housed in separate air-conditioned rooms (12-hour dark/light cycle) at 20°C and a humidity of 53%. Experiments were performed in agreement with the European Communities Council Directive of 24 November 1986 (86/609/EEC) on the ethical use of animals and were approved by the local ethical committee at Karolinska Institute.

Unilateral 6-OHDA-lesioning of nigral DA axons was performed as previously described (Zhang, Andren, Greengard, & Svenningsson, 2008). Briefly, rats were anesthetized with ketamine (80 mg/kg, intraperitonial (i.p.)); Parke-Davis, Boxmeer, Netherlands)/xylazine (10 mg/kg, i.p.; Bayer, Kiel, Germany), pretreated with desipramine (25 mg/kg, i.p.; Sigma, Stockholm, Sweden) and pargyline (5 mg/kg, i.p.; Sigma), placed in a stereotaxic instrument and injected with 6-OHDA (2.5 µl of a 5 mg/ml solution; Sigma) into the medial forebrain bundle of the right hemisphere (AP: −2.8 mm, ML: −2.0 mm and V: −9.0 mm). Two weeks after unilateral 6-OHDA-lesioning, rats were administered with apomorphine (1 mg/kg, i.p; Sigma), and their contralateral rotations were measured over 30 minutes. Another four weeks later, both control rats and the 6-OHDA-lesioned rats were sacrificed by decapitating, using a guillotine. The unilaterally sham-lesioned rats were treated in the same way as 6-OHDA-lesioned rats except saline was used instead of 6-OHDA. Rats were decapitated according to the method of Zhang et al (Zhang et al., 2008). Brains were quickly removed and put in a cup of isopentane (2-methylbutan 99% solution) on dry ice for 15-20 seconds and subsequently wrapped in tin foil. The brains were stored in -80°C until further use.

Figure 3. Leica cryostatmitocrome.

The rat brains were sectioned using a Leica cryostatmitocrome (Figure 3). Coronal sections of the rat brain were cut at a thickness of 12-14 µm. After cutting, the tissues were transferred by thaw mounting onto conductive ITO slides (Bruker

Daltonics, Bremen, Germany) prior to storage at -80°C. The tissue samples intended to be analyzed were transported from the freezer on dry ice and inserted into a desiccator. They were desiccated for 15 minutes prior to further sample preparation.

3.3.2 Washing preparation

The washing preparation was performed with ammonium acetate in two concentrations, 50 mM and 100 mM.

The tissue sections intended to wash were submerged in buffer solution and held stationary for 10 seconds. The glass slide was then removed from the buffer and big drops of liquid blotted away with care taken not to touch the tissue.

The tissue section was then completely dried under high vacuum for 15 minutes.

While optimizing the washing preparation was performed on slides containing four tissue sections, two sets of control rat brain sections and two sets of sham-lesioned rat brain tissue. They were placed so that half of the slide could be submerged and each half would contain one control rat brain tissue section and one sham-lesioned rat brain section, for the comparison of signals between each set of brain tissue (S05, S06, S10, S11, S12).

Once optimized, the whole slide was submerged with all the sections it contained (S11, S12).

3.3.3 Derivatization of cholesterol

The preparation of two different solutions containing BA were as follows: 5 mg of BA was dissolved in 200 µL of water and kept in a refrigerator as a stock solution before adding it to the spray solution for slides S07 and S08; another 5 mg of BA was dissolved in 1200 µL consisting of 8/3/1 (acetonitrile (ACN)/water/dimethylformamide (DMF)) and split into 12 aliquots each containing 100 µL of the BA solution and kept in a freezer at -18°C as a stock solution before being added to the spray solutions for slides S09-S12. Two different application systems were tested for BA addition to the tissue.

3.3.3.1 TLC sprayer application of BA

The sprayer used was a Kontes TLC reagent sprayer (Figure 4). The TLC-sprayer is a manual sprayer that utilizes nitrogen flow to nebulize the solution added to the spray beaker. The nitrogen flow was set to 3 bars of pressure and BA in its solvent system was added to the spray beaker and deposited onto the slide held at half an arm's length. After each set of adding BA onto the tissue the nitrogen flow was used to dry the sample. This resulted in a fairly wet application on the tissue sample. The solvent system utilized in the TLC sprayer was 50/50 ACN and water. This spray solvent had 50 µg/mL concentration of BA and 5 mL was sprayed using the TLC sprayer.

Figure 4. Kontes TLC sprayer.

3.3.3.2 ImagePrep machine application of BA

The reaction was applied to the tissue segment using the ImagePrep (ImagePrep, Bruker Daltonics) device (Figure 5). The ImagePrep is an automated vaporizer that uses vibrations to vaporize the solvent onto the tissue which is situated in a spray chamber. The spray process can be controlled by changing the options of how long the process should take, nebulizer power, nebulizer modulation, nebulizer spray time, incubation period and drying time. Each option can either be left up to the machine to automatically detect or manually choose. In this case all the options were manually chosen. The total deposition process was set at 60 cycles or when the spray solution was finished. The nebulizing options were set at 16-18% power, 20% modulation and 2.5 second spray time. The incubation period was set to 15 seconds and the drying time to 70-75 seconds.

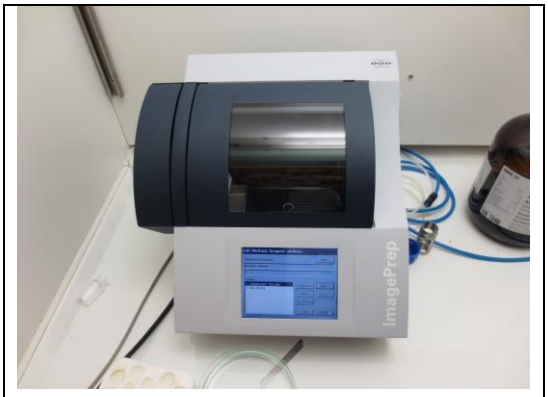

Figure 5. ImagePrep automated vaporizer.

For the ImagePrep application a BA solvent system with ACN/ water/DMF was chosen with the proportions 8:3:1, same as previously used for cholesterol derivatization

(Wu et al., 2009). The reaction solution (2 mL) was inserted into the spray beaker of the ImagePrep machine. Two concentrations of BA were tested, 126 μg/mL (S08-S10) and 63 μg/mL (S11).

3.3.4 Matrix application

The matrix application was performed with three different methods: dry sieve coating, wet application with TLC-sprayer and wet application with TM-sprayer (HTX Technologies, North Carolina, USA). The matrix used was DHB (50 mg/mL). In the wet applications the spray solution was comprised of ANC/water (50/50) with 0.2% trifluroacetic acid (TFA).

3.3.4.1 Dry matrix application

Dry matrix application using a sieve to deposit the DHB matrix on the samples was tested. The matrix was finely ground up and put in a sieve with very small holes and shaken, distributing small flakes of DHB onto the sample. The sample was then tapped on the side to remove excess matrix. The process was repeated for five sets of coating followed by drying with nitrogen gas and then another five sets of coating. Care was taken not to bank the sample always on the same side as to even out the distribution of matrix.

3.3.4.2 TLC-sprayer

A TLC-sprayer was used to coat the sample with matrix. The process of using the TLC-sprayer was performed in the same was as reactant application, described above, except the sample was held at an arm's length instead of half an arm's length.

3.3.4.3 HTX TM-sprayer

The TM-sprayer (Figure 6) is an automated matrix sprayer which transfers heat to the matrix solution in order to increase absorption into the tissue sample. It also uses controlled flow of nitrogen to focus the spray and drying time. The sprayer has fully controllable configurations such as the heat delivered to the matrix, size of the area to be sprayed, velocity of the spray nozzle, how many passes of spraying and flow of matrix. The settings used in this experiment were a temperature of 85°C, normal glass slide area (75 mm x 25 mm, 10 mm all around margin), velocity of 1200 mm/min, four passes of spraying with 3 mm of track spacing and the 3rd and 4th pass were offset by 1.5 mm and 0.1 mL/min flow of matrix.

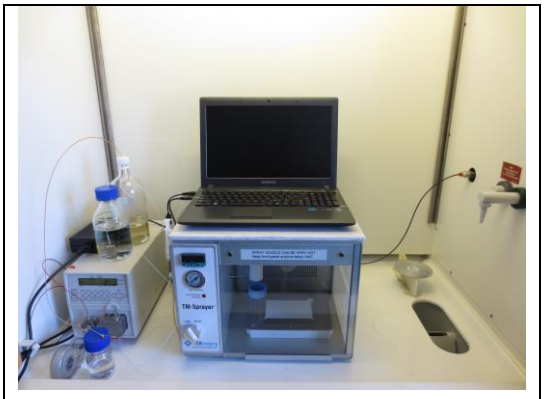

Figure 6. TM automated sprayer.

3.3.5 MALDI-MSI analysis

Before analysis, using MALDI-MSI, an optical image was taken with a flatbed scanner, marks were added for triangulation.

The MALDI-MSI analysis of samples was performed using a reflectron geometry MALDI TOF-TOF mass spectrometer (Ultraflextreme, Bruker Daltonics, Bremen, Germany) (Figure 7) in positive ion mode using a Smartbeam II laser, 355nm wavelength. Different spatial resolution was used ranging from 100-200 μm. The parameters for mass spectrometry were set as follows: ion source 1, 25.05 kV; ion source 2, 22.41 kV; lens voltage, 7.05 kV; gain factor, 5.1x; matrix suppression mass was set to off; laser spot size put to small; frequency was set at 2000 Hz; reflector 1, 26.55 kV; reflector 2, 13.42 kV; realtime smoothing 2 GS/s. The imaged regions were selected prior to running the analysis and were not always in the same order as to try to

Figure 7. The Ultraflextreme MALDI-TOF-TOF analyzer.

prevent bias arising from factors such as matrix degradation or variation in the mass spectrometer sensitivity. The laser intensity was optimized at the start of each individual run.

Tandem mass analysis of samples were performed utilizing the laser induced dissociation (LID) combined with LIFT MS/MS technique on the MALDI TOF-TOF mass spectrometer (Bruker, Daltonics) (Suckau et al., 2003). The parent ion mass was set prior to running the analysis and a precursor ion selector (PCIS) window range set at 0.66% of parent mass. Two different spatial resolution parameters were used, 100 µm and 150 µm. The parameters of the MS/MS analysis were as follows: ion source 7.53 kV; ion source 2, 6.74 kV; lens voltage, 3.63 kV; gain factor, 8.6x; laser spot size put to medium; frequency was set at 1000 Hz; reflector 1, 29.66 kV; reflector 2, 14.03 kV; realtime smoothing set to off; LIFT 1, 18.98 kV; LIFT 2, 4.2 kV. The measurement regions were selected prior to running and the laser intensity was optimized before starting each individual run. The data was analyzed using FlexImaging version 3.0

3.3.6 Overview

Table 3. Overview of sample preparation on different slides

Slide	Resolution [µm]			Matrix application			Reagent application		Washing [mM]		Figure
	100	150	200	Dry	TLC	TM	TLC	ImagePrep	50	100	
S01	X			X							8
S02	X				X						8,24
S03	X				X						9
S04			X		X				X		10,11,12,13
S05		X			X					X	14,15,16
S06	X				X		X				17
S07		X			X		X				18
S08			X		X			X			19,20
S09		X				X		X		X	21,22,23,24
S10	X					X		X		X	25
S11	X					X		X		X	26

4. RESULTS

4.1 Sample preparation method development

4.1.1 MALDI-MSI without sample preparation method

The MALDI-MSI analysis of cholesterols relative abundance and distribution was first tested with dry matrix application and then with wet application of DHB using the TLC sprayer.

The results from these runs on slides S01 and S02 can be observed in Figure 8 The signal for dry application is adequate but the overall signals from other elements in the spectrum are quite low. The distribution of the cholesterol in slide S01 is not specifically localized. Examining the MALDI-MSI results from slide S02 depicted in Figure 8 a distribution pattern is noticed. The results using the same preparation as slide S02 were difficult to recreate consistently as can be seen in Appendix I (showing the other analyses trying to use the same solvent system). The overall average signal intensity of cholesterol for slide S01was 35 a.u. and about 3 a.u. for slide S02.

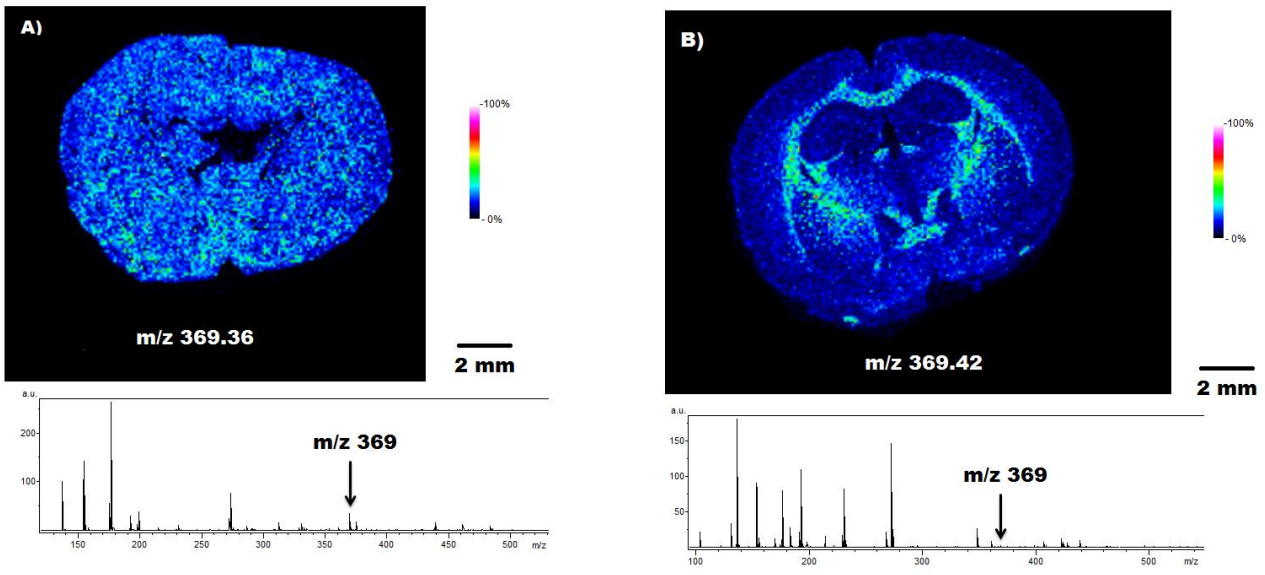

Figure 8. MALDI-MSI relative abundance and distribution of cholesterol testing different matrix applications without prior sample preparation. Showing the results from slides S01 and S02. A) Slide S01 utilized dry application of the DHB matrix B) Slide S02 utilized wet application of 50 mg/mL DHB in 50% ACN with 0.2% TFA. Image and spectra are TIC normalized.

When tandem MS analysis was performed on slide S03, which was processed in the same way as slide S02 but with an added cholesterol standard spot, the cholesterol fragments were detected in the cholesterol standard spot and in tissue, but with lower signal. The resulting MS/MS spectrum is shown in Figure 9. This spectrum shows the major fragments associated with cholesterol fragmentation, such as the 161 peak, 147 peak, 109 peak and the 95 peak. The fragments could mainly be visualized from the cholesterol standard but the fragment distribution on tissue was difficult to assess.

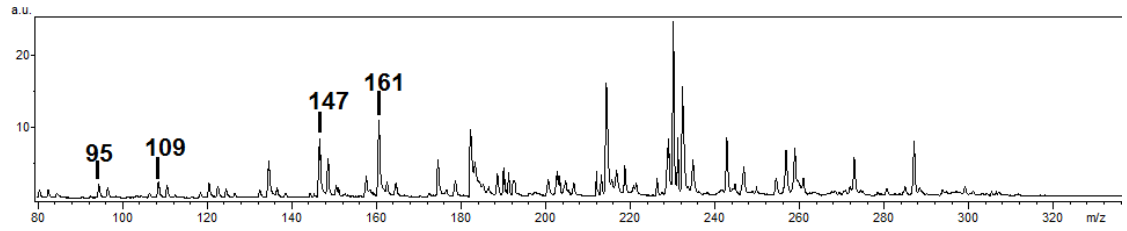

Figure 9. MALDI tandem mass spectra of the 369 peak from slide S03, indicating the peaks associated with cholesterols major fragments.

4.1.2 MALDI-MSI with washing method

4.1.2.1 Washing with 50 mM ammonium acetate

Figure 10. Overview of slide S04 before analysis by MALDI-MSI. Showing the white marks used for triangulation

Figure 10 gives an overview of slide S04 after washing, but before running analysis using MALDI-MSI. Figures 11, 12 and 13 are all depicting results from the same run on slide S04. In Figure 11 the MALDI-MSI abundance and distribution of cholesterol is compared between duplicate sets of tissue where one set went through the washing protocol using 50 mM ammonium acetate buffer solution and the other one did not. A direct comparison is made between the same tissue sets, the control sections in Figure 12 and the sham-lesioned sections in Figure 13.

In Figure 12, a direct comparison of the effect washing has on the cholesterol signal in control samples is made. The yellow spectrum line corresponds to the washed tissue and the red spectrum to the unwashed sample. An increase in signal is detected in the washed control sample and the washing preparation can be roughly estimated to increase the signal from 3.5 a.u. to 5 a.u. in intensity. Washing increased the cholesterol signal in control tissue by a factor of 1.4.

The same comparison is made with washed and unwashed sham lesioned tissue in Figure 13. Here the pink spectrum belongs to the washed sample and green spectrum the unwashed spectrum. The cholesterol signal goes from roughly 3.5 a.u. to about 4.5 a.u. by washing the sham lesioned segment with 50 mM ammonium acetate buffer. This is a factor of 1.3.

This experiment that utilized the washing preparation with 50 mM ammonium acetate solution increased the cholesterol signal by an average of 1.4 over the two tissue sample sets.

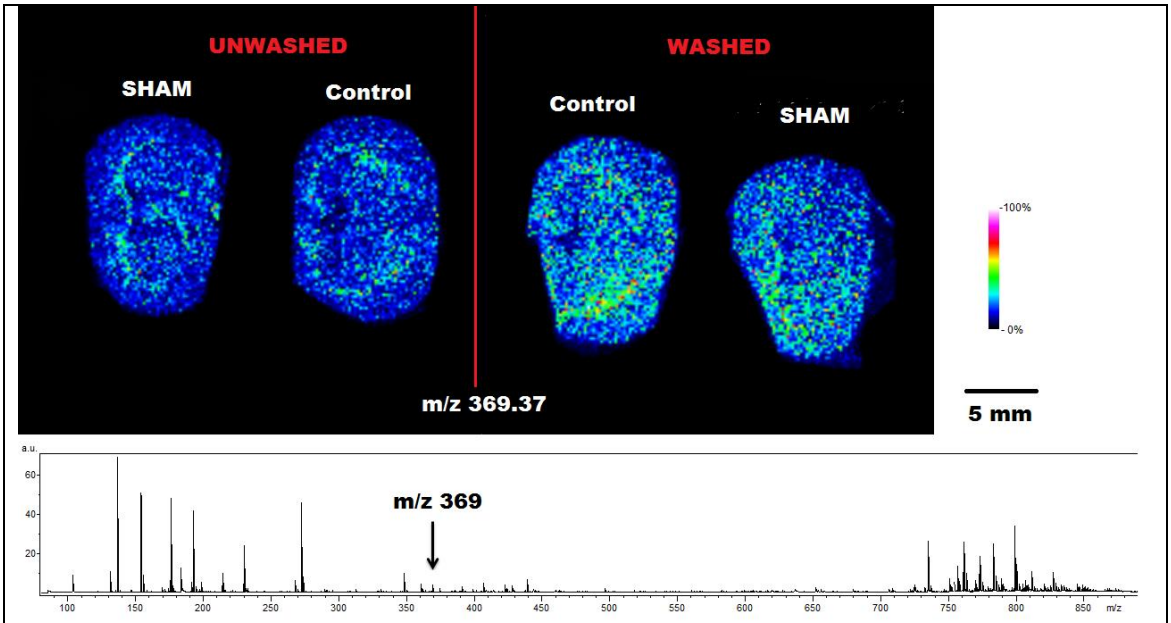

Figure 11. Whole image analysis of slide S04 with duplicate sets of sham and control tissue where one set, on the right side, has been washed with 50 mM ammonium acetate buffer. The red line depicts the separation of washed and unwashed tissue. The overall average spectrum for the collected image is depicted underneath. Image and spectrum are TIC normalized.

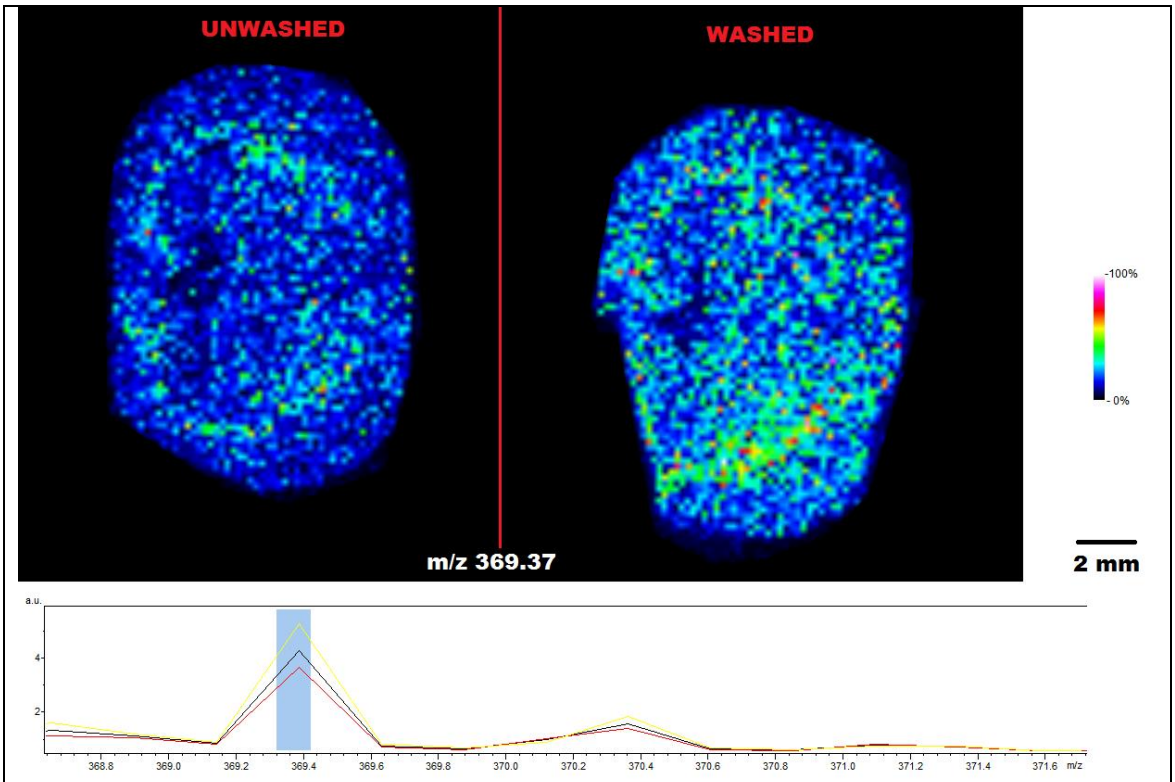

Figure 12. Slide S04, directly comparing the difference in spectra and intensity of signal in the image between control samples in the washing experiment. The yellow spectrum belongs to the washed control sample and the red spectrum the unwashed one. Black spectrum is the analysis overall average spectra. Image and spectra are TIC normalized.

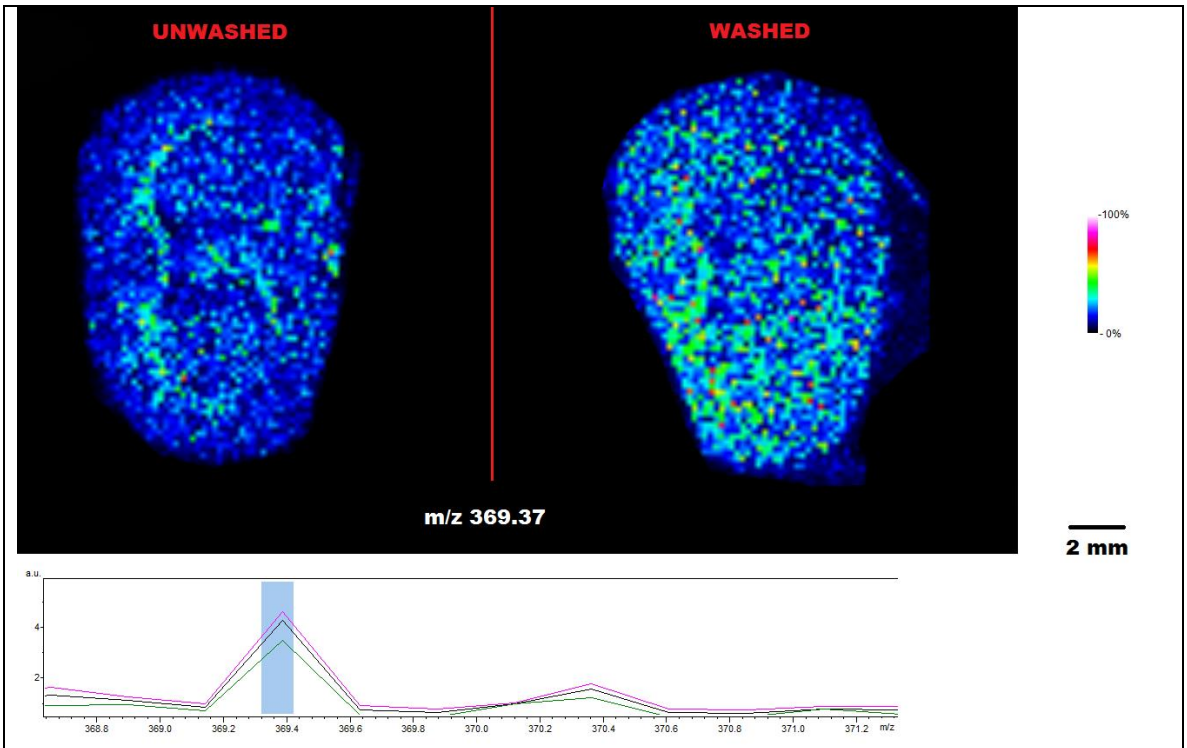

Figure 13. Slide S04, directly comparing the difference in spectra and intensity of signal in the image between sham-lesioned samples in the washing experiment. The pink spectrum belongs to the washed sham sample and the green spectrum the unwashed one. Black spectrum is the analysis overall average spectrum. Image and spectra are TIC normalized.

4.1.2.2 Washing with 100 mM ammonium acetate

An increased concentration of the washing buffer was tested. In this washing preparation 100 mM of ammonium acetate was used as the washing solution. Figure 14 shows the overall MALDI-MSI results from slide S05 when looking at relative abundance and distribution of cholesterol with and without washing. The red line depicts where the washing solution reached. It is worth noting that because of a misstep in performing the washing method the washing solution did not cover the whole sham-lesioned segment that was intended to be submerged in the washing solution. The overall spectrum from the analysis is shown in Figure 14. A more close comparison is made in Figures 15 and 16 comparing the efficiency of the washing between the set of control tissue and the sham-lesioned set.

In Figure 15, a direct comparison is made of the MALDI-MSI relative abundance and distribution of cholesterol with and without the washing preparation on control samples from slide S05. The figure shows that the signal is increased with the 100mM ammonium acetate washing method. The signal intensity of each spectrum can be roughly estimated. The unwashed segment has the signal intensity of 3.1 a.u. that is increased in the washed segment to 7.1 a.u., which is a factor of 2.3.

Figure 16 compares the sham-lesioned sections from the same slide. Again the washed tissue has higher intensity of the cholesterol peak. When comparing the spectrum of the tissues the washed segment has 6.9 a.u. and the unwashed 3.8 a.u., which is an increase by a factor of 1.8.

Using the 100 mM ammonium acetate buffer as the washing solution increased the signal of cholesterol by an average of 2.1 over the two tissue sample sets.

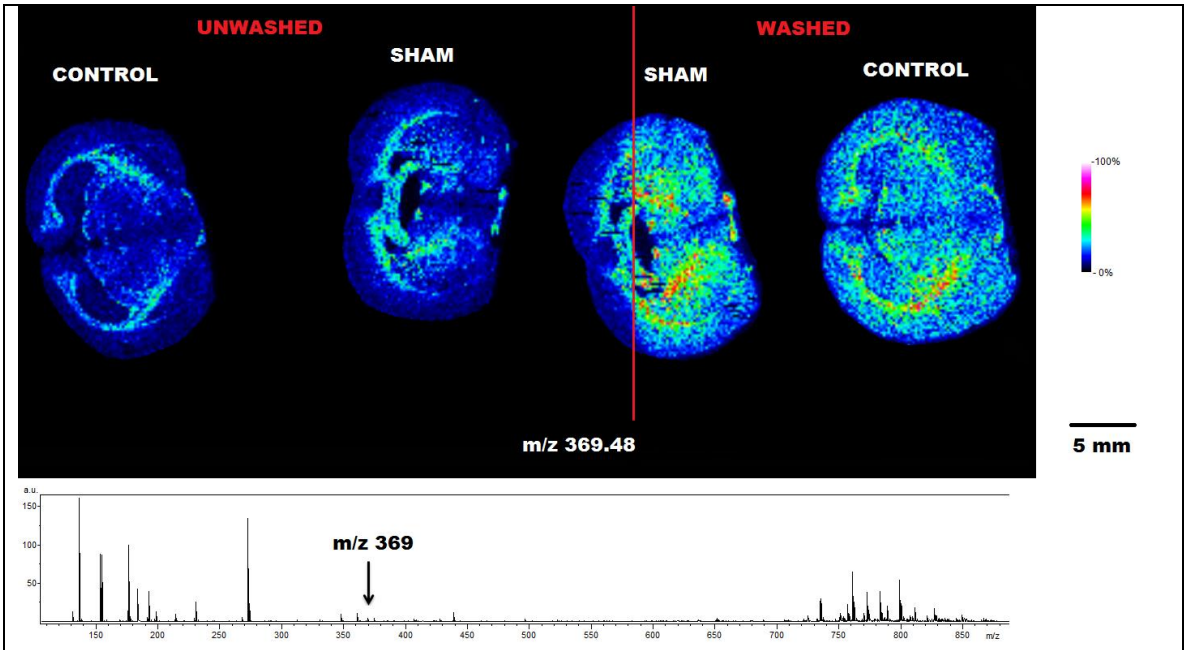

Figure 14. Whole image analysis of slide S05 with duplicate sets of sham and control tissue where one set, on the right side, has been washed with 100 mM ammonium acetate buffer. The red line depicts the separation of washed and unwashed tissue. The overall average spectrum for the collected image is depicted underneath. Image and spectrum are TIC normalized.

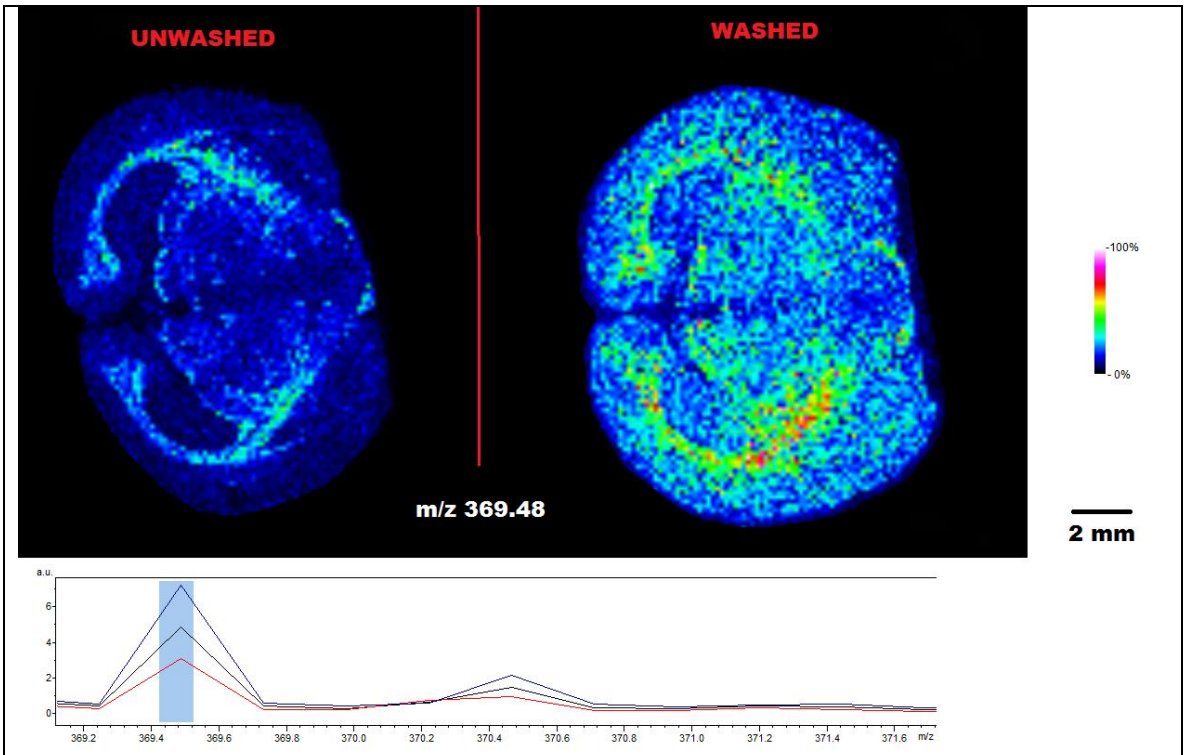

Figure 15. Slide S05, directly comparing the difference in spectra and intensity of signal in image between control samples in the washing experiment. The blue spectrum belongs to the washed control sample and the red spectrum the unwashed one. Black spectrum is the analysis overall average spectrum. Image and spectra are TIC normalized.

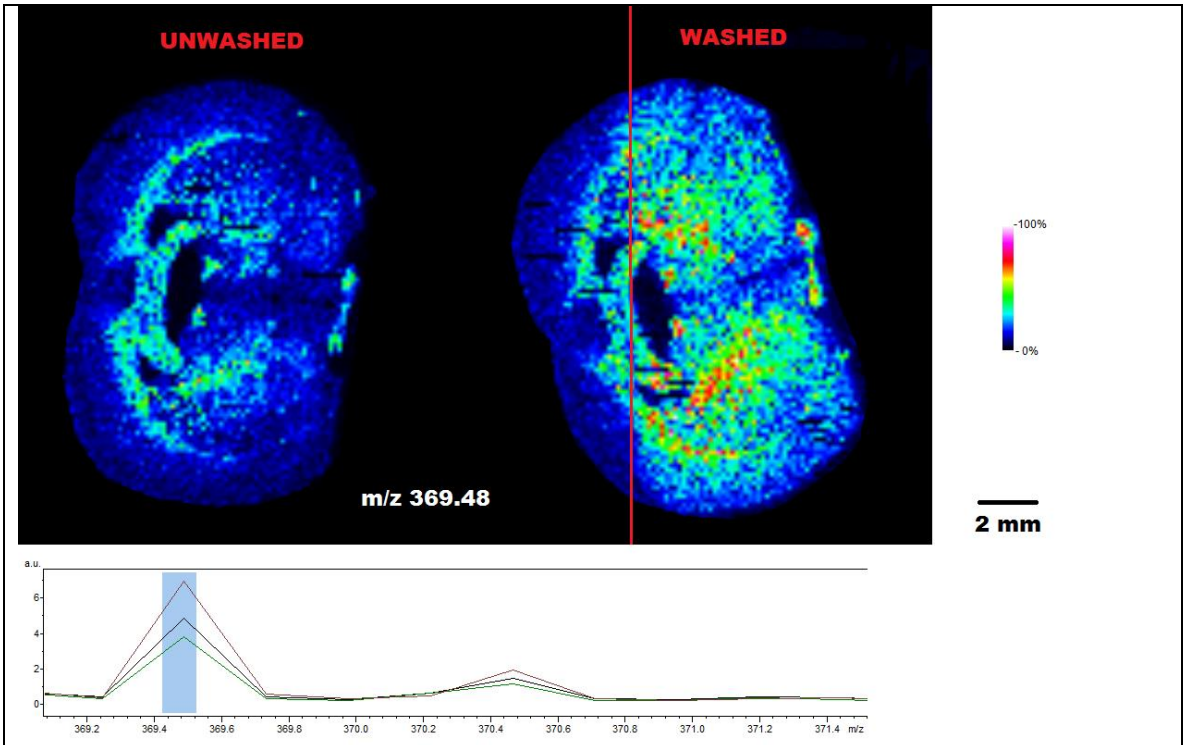

Figure 16. Slide S05, directly comparing the difference in spectra and intensity of signal in the image between the sham-lesioned samples in the washing experiment. The brown spectrum belongs to the washed sham sample and the green spectrum the unwashed one. Black spectrum is the analysis overall average spectrum. Image and spectra are TIC normalized.

4.1.3 MALDI-MSI using derivatization method

In order to increase cholesterol ionizability, BA was utilized to react with cholesterol and charge label it. The reaction was first tested with a dropper (Appendix II). The derivatized cholesterol peak in the spectrum is located at m/z 488 and the results of the utilization of the derivatization sample preparations on slides S06, S07 and S08 are shown in Figures 17, 18 and 19 respectively. The difference between the MALDI-MSI experiments in these figures is that slides S06 and S07 utilize the TLC-sprayer for deposition on samples, slide S07 depositing BA in a drier manner, holding the manual sprayer further away from the tissue sample sections than slide S08. In figure 19 the BA reactant was sprayed on the sample using an automated sprayer, ImagePrep. Figure 17 shows the relative abundance and distribution of the newly formed cholesterol derivative peak at 488.4. The signal intensity in slide S06 is roughly 115 a.u.

In Figure 18 the relative abundance and distribution of the cholesterol derivative is shown on slide S07. Signal is seen off-tissue. The overall average signal intensity of the derivative peak from this run was about 65 a.u.

The automated vaporizer ImagePrep was utilized to disperse the reaction solvent on slide S08. The result of this analysis is shown in Figure 19. This MALDI-MSI analysis used a higher concentration of BA, 126 µg/mL compared with 50 µg/mL used in previous reaction analysis. The signal from the cholesterol derivative is increased compared with slides S07 and S06 and is approximately 164 a.u.

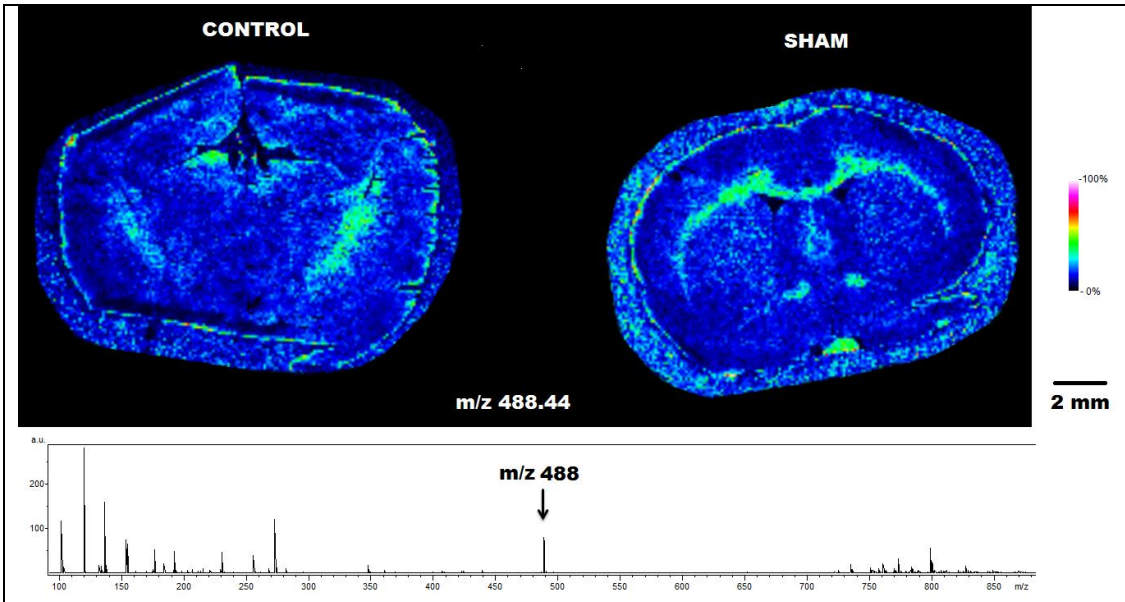

Figure 17. Slide S06, MALDI-MSI relative abundance and distribution of the cholesterol derivative peak (m/z 488) on control and sham-lesioned samples. The TLC-sprayer was used to deliver the reactant at a concentration of 50 µg/mL. The overall average spectrum is depicted underneath. Image and spectrum are TIC normalized.

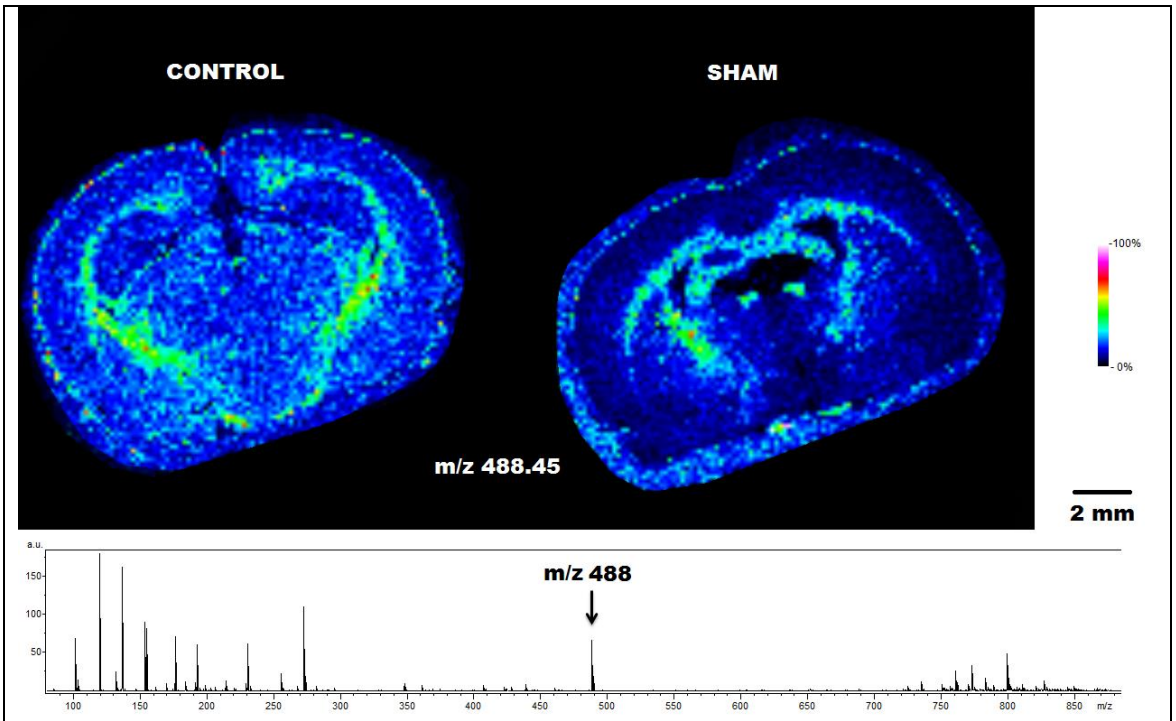

Figure 18. Slide S07, MALDI-MSI relative abundance and distribution of the cholesterol derivative peak (m/z 488) on control and sham-lesioned samples. The TLC-sprayer was used to deliver the reactant at a concentration of 50 µg/mL. The overall average spectrum is depicted underneath. Image and spectrum are TIC normalized.

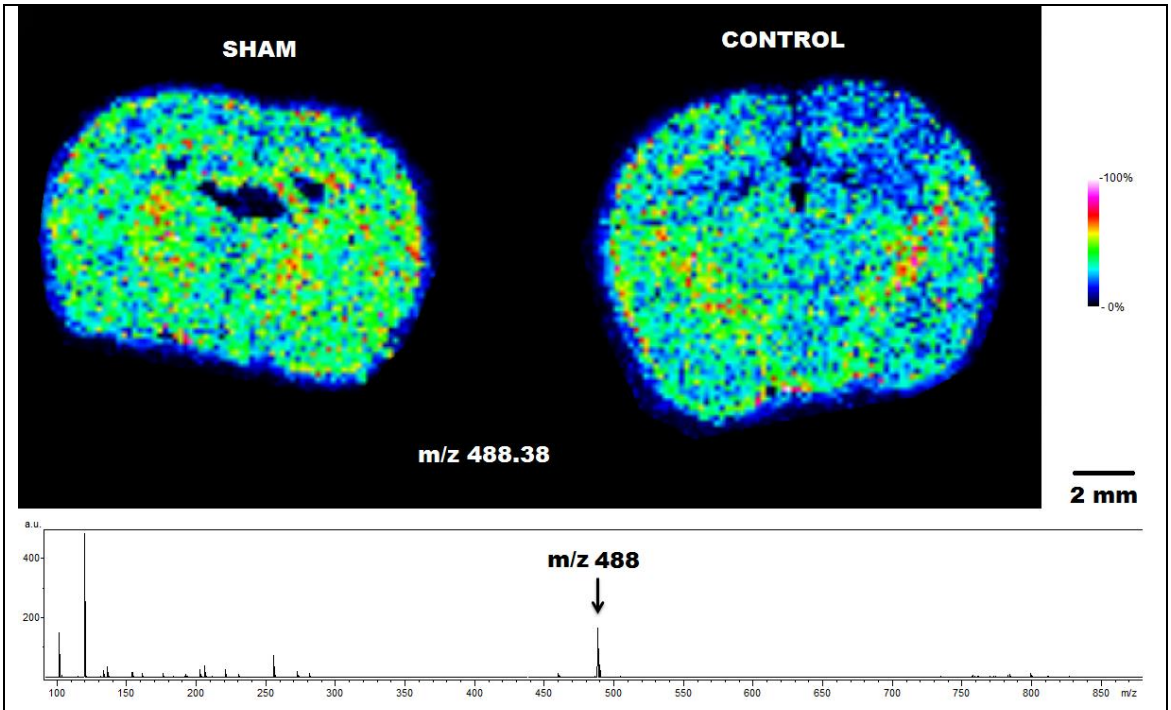

Figure 19. Slide S08, MALDI-MSI relative abundance and distribution of the cholesterol derivative peak (m/z 488) on control and sham-lesioned samples. The ImagePrep-sprayer was used to deliver the reactant at a concentration of 126 µg/mL. The overall average spectrum is depicted underneath. Image and spectrum are TIC normalized

4.1.3.1 Tandem mass analysis after derivatized preparation

The collection of MSMS data was performed on slide S08 after the BA preparation and MALDI-MSI analysis. Figure 20 depicts the major fragments of cholesterol and the BA, where the 102 peak is formed from the ionized BA fragment and 120 peak is the ionized BA and water adduct.

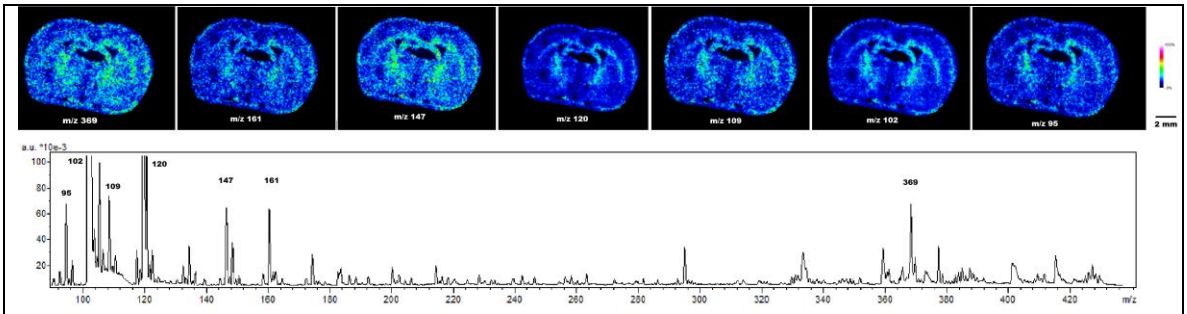

Figure 20. Tandem MS data for slide S08 performed after MALDI-MSI analysis. The major peaks of the fragments associated with derivatized cholesterol are highlighted in the spectra and their associated image shown above.

4.1.4 MALDI-MSI of combined method

Figure 21 compares tissue sections that went through the washing preparation with 100 mM ammonium acetate buffer prior to reaction preparation with BA and duplicate set that went unwashed before reaction preparation on slide S09.

When the same duplicate of tissue is compared directly we get Figures 22 and 23. Figure 22 compares the results from the set of control rat brain tissues from the same slide S09 in Figure 21. Considerably higher signal is seen when the tissue sample is first washed and then applied with the BA reactant preparation then without prior washing preparation. The average spectrum signal of the cholesterol derivative in the washed control tissue can be estimated to be 470 a.u. compared with 115 a.u. of the unwashed tissue. This is a signal increase by a factor of 4.1.

The differences for the duplicates of sham-lesioned tissues are shown in Figure 23. The signal intensity of the derivatized cholesterol is 480 a.u. for the prior washed sham-lesioned section compared with 174 a.u. for the unwashed tissue section. This is a signal increase by a factor of 2.8.

The results from this experiment is that prior washing preparation before using the derivatization step causes an average increase in the derivatized cholesterol peak over the two tissue sets by a factor of 3.4.

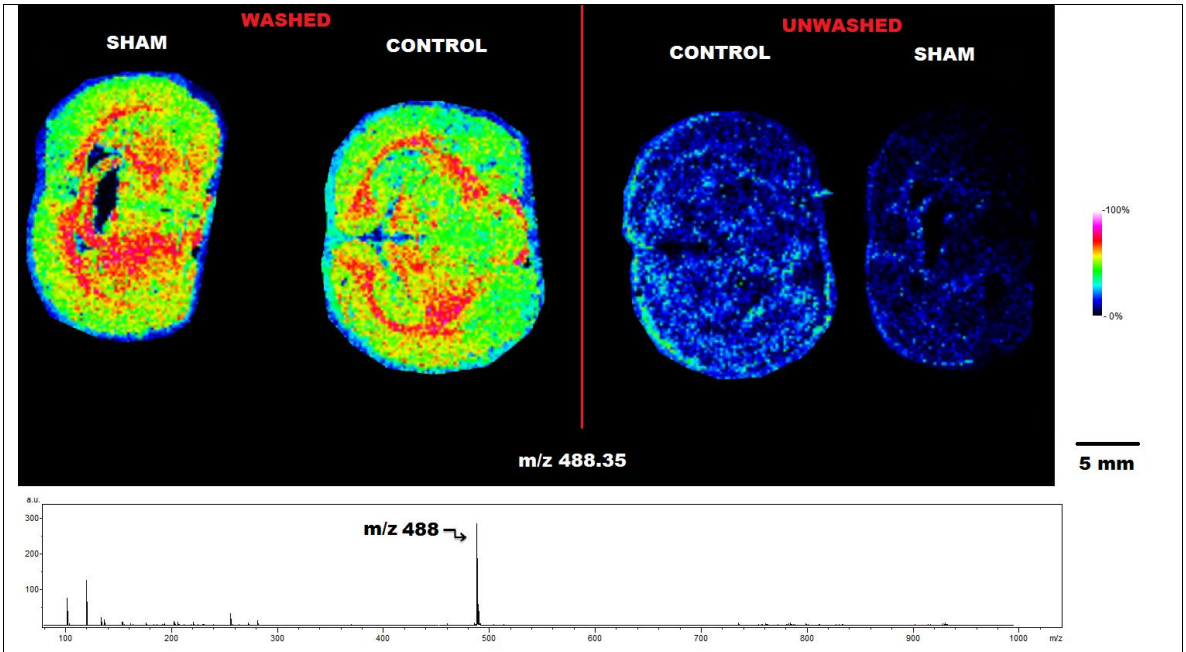

Figure 21. Whole image analysis of slide S09 with duplicate sets of sham and control tissue where one set, on the left, has been washed with 100 mM ammonium acetate buffer prior to the derivatization of the whole slide. The red line depicts the separation of washed and unwashed samples. Image shows the relative abundance and distribution of the derivatized cholesterol peak (m/z 488) and the overall average spectrum is depicted underneath. Image and spectrum are TIC normalized.

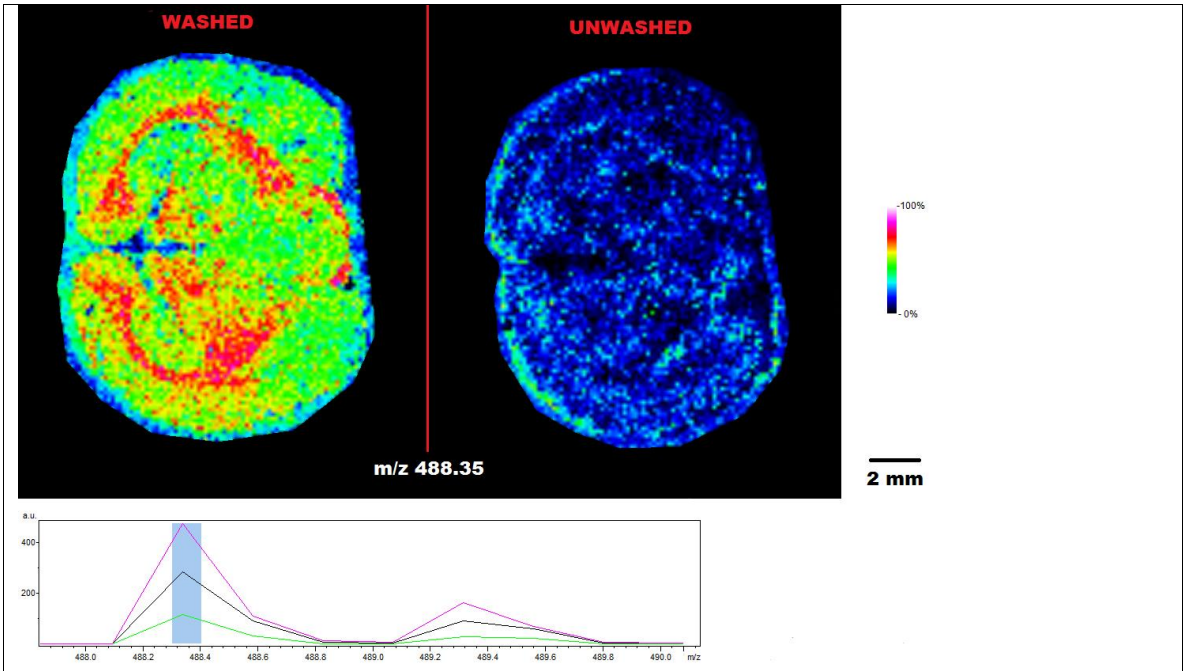

Figure 22. Slide S09, directly comparing the difference in spectra and intensity of signal in the image between control samples in the washing and reacting experiment. The pink spectrum belongs to the washed control sample prior to reaction and the green spectrum the unwashed one. Black spectrum is the analysis overall average spectra. Image and spectra are TIC normalized.

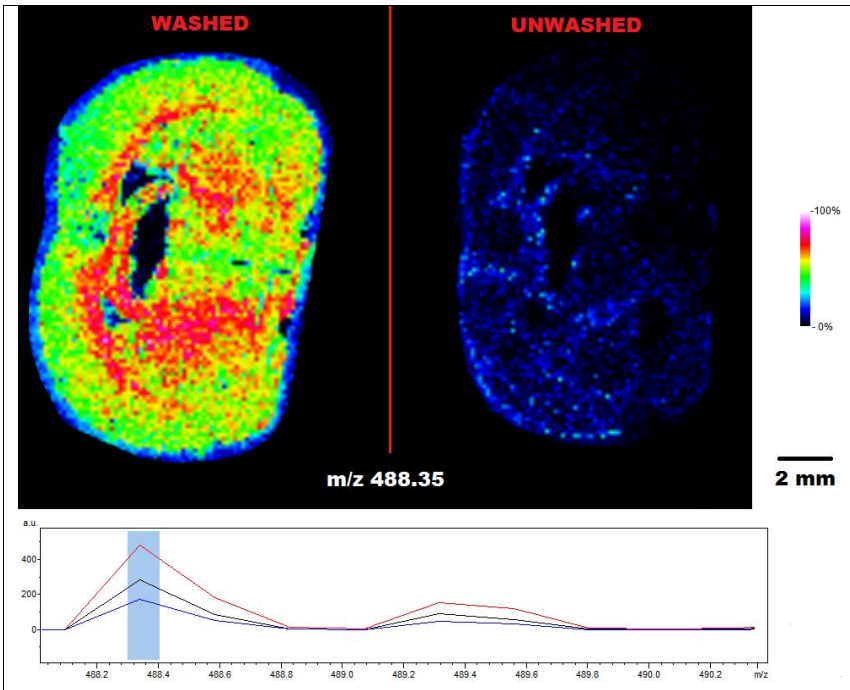

Figure 23. Slide S09, directly comparing the difference in spectra and intensity of signal in the image between sham-lesioned samples in the washing and reacting experiment. The red spectrum belongs to the washed control sample prior to reaction and the blue spectrum the unwashed one. Black spectrum is the analysis overall spectrum. Image and spectra are TIC normalized.

Figure 24 depicts the change in signal intensity from spectra of the control tissues from slides S02, which the combined sample preparation was not performed on, and S09, with the developed sample preparation method. The signal intensity was increased from 3.2 a.u. to 472 a.u. which is a factor of 148.

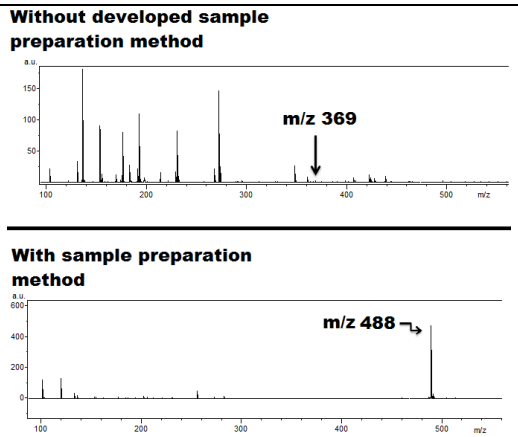

Figure 24. Comparison of signal intensity between cholesterol without the new sample preparation method (control tissue from slide S02) and with the new developed sample preparation method (control tissue from slide S09). Spectra is TIC normalized

4.2 Implementation of the newly developed method on PD-model brain tissue

The optimized combined method was then used to diagnose the tissue model on slides S10 and S11 for Parkinson's disease. This developed method was utilized on two different sample slides containing the PD-model and sham and control tissue in Figures 25 and 26 respectively. In these slides the matrix coating was performed by the TM-sprayer. The only difference between the slides S10 and S11 is that the former one uses the BA concentration of 126 µg/mL compared with 63 µg/mL in slide S11. The results from these experiments show a high signal for the derivatized cholesterol peak and the relative abundance in tissue is high but an apparant difference in relative abundance between lesioned and unlesioned side of the PD-model is not noticed. The overall average signal intensity of the derivative is 515 on slide S10 and 351 a.u. on slide S11.

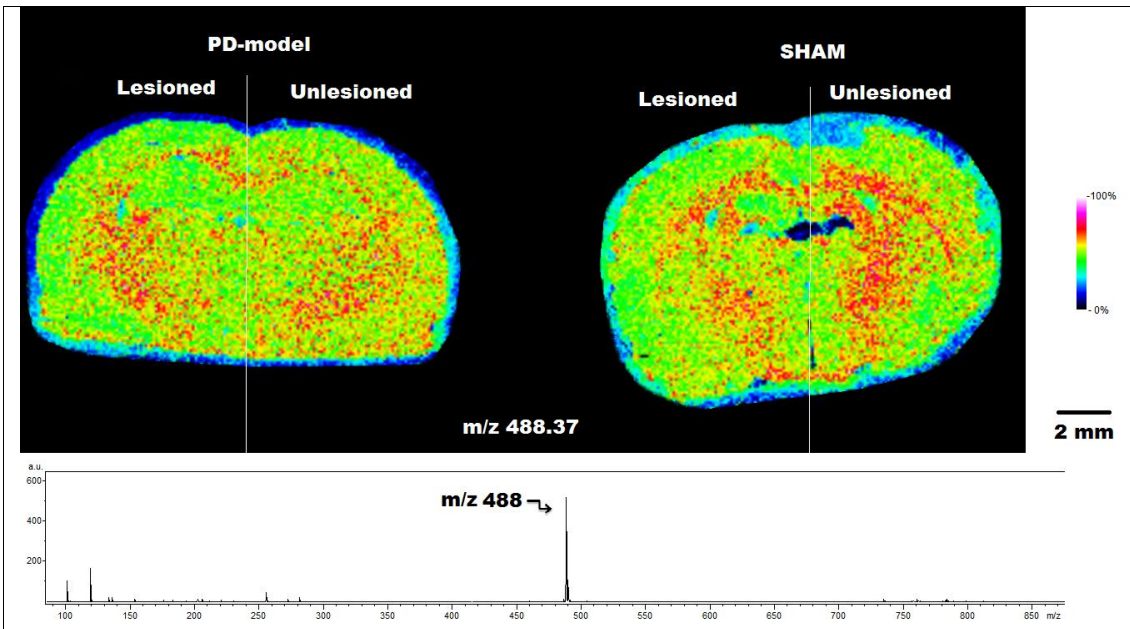

Figure 25. Slide S10, MALDI-MSI relative abundance and distribution of the cholesterol derivative peak (m/z 488) on PD-model and sham-lesioned samples. The ImagePrep-sprayer was used to deliver the reactant at a concentration of 126 µg/mL followed by matrix coating by the TM-sprayer. The overall average spectrum is depicted underneath. Image and spectrum are TIC normalized

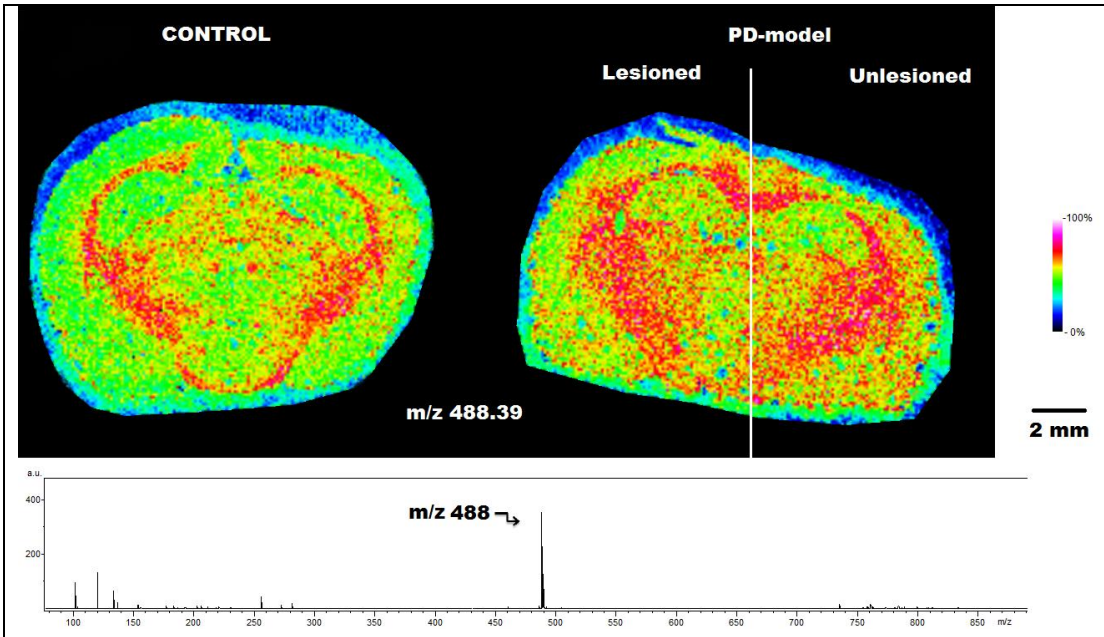

Figure 26. Slide S11MALDI-MSI relative abundance and distribution of the cholesterol derivative peak (m/z 488) on PD-model and sham-lesioned samples. The ImagePrep-sprayer was used to deliver the reactant at a concentration of 63 µg/mL followed by matrix coating by the TM-sprayer. The overall average spectrum is depicted underneath. Image and spectrum are TIC normalized

5. DISCUSSION

5.1 Development of the method

Cholesterol is, as described before, a difficult molecule to ionize due to its low proton affinity and shortage of functional groups (Wu et al., 2009). The task was therefore to develop a sample preparation method for the detection and identification of the molecule using the MALDI-MSI tool. As cholesterol is an abundant endogenous substance within the brain, (Liu et al., 2010), located in membranes and in high amounts in the myelin sheaths, the relative abundance would be expected to be substantial in all areas of the brain tissue with higher amounts in brain areas constructed mainly of myelin sheaths, such as the corpus callosum and a part of the striatum (Dietschy & Turley, 2004; Trim et al., 2008; Veloso et al., 2011). Notice must be taken that brain sections from different brains are not taken at the same depth level and so visualization of the major brain structures varies when looking at the control and sham-lesioned rat brain sections for instance.

A signal can be seen using the dry matrix application (Figure 8, A), however distinct distribution pattern is lacking. This could be because co-crystallization of matrix with the molecule of choice is needed for more efficient ionization of the molecule and cholesterol was not being extracted into crystallizing efficiently with the dry matrix (Goto-Inoue et al., 2011). For this reason a wet application of the matrix was tested. With the use of wet spraying of the matrix a definite distribution pattern could be noticed (Figure 8, B) but the intensity was so low that no relative abundance could be measured outside the structures comprising highest amount of the molecule, the striatum and corpus callosum (Dietschy & Turley, 2004; Trim et al., 2008; Veloso et al., 2011). In addition, when identifying cholesterol using tandem mass spectrometry of the parent peak (m/z 369.35), the signal was too weak for proper visualization of the spatial distribution on tissue. Due to these facts an increase in sensitivity was required, thus calling for additional sample preparation steps.

The first sample preparation step to address was washing of the tissue in order to remove salts and other contaminants that are likely to suppress ionization. For this purpose a buffer solution containing ammonium acetate was chosen. Washing

preparation with this buffer had previously been described both to increase the signal of small mole weight substances (Shariatgorji et al., 2012) and also in an effort to increase the signals from lipids (Angel et al., 2012). The requirement of this preparation step is that the molecule of interest should not be soluble in the washing solution, otherwise it may be removed or delocalized with the washing before the analysis (Shariatgorji et al., 2012). For cholesterol this is probably less of a factor as the molecule is insoluble in aqueous solvents (Davis et al., 1989). For the comparison of the improved signal intensity, slides with four tissue sections were used; two control brain tissues and two sham lesioned brain tissues. The order of the tissues was such that when half the slide went through the washing preparation one control and one sham sections were washed leaving the other pair unwashed. It was important to compare the effect directly on the same slide to avoid between-run differences that might occur in the mass spectrometer. In addition, sections were cut consecutively for enhanced comparison. The buffer was prepared at two concentrations, 50 mM and 100 mM with ammonium acetate in water. The prior experiment using the washing preparation to increase the signal for lipids had described cracking of the tissue when using a concentration higher than 75 mM (Angel et al., 2012). However, as washing with 50 mM buffer solution only rendered an average increase of signal by a factor of 1.4, not even doubling the signal, and the article using washing preparation on small mole weight molecules had used 100 mM (Shariatgorji et al., 2012) this concentration was also tested. This gave roughly two times the original signal in average over two tissue sets. The washing step did not seem to alter the distribution in any major way, only increase the relative abundance so more can be visualized outside the areas inhibiting the most amount of cholesterol. Although the washing step resulted in a fair increase of signal, the overall signal was still too low for adequate MS/MS to be performed. Hence, further sample processing was required.

Experiments where cholesterol is reacted with a chemical to aid its ionization has been performed before, both in mass spectrometry such as ESI (Johnson et al., 2001; Liebisch et al., 2006; Sandhoff et al., 1999) and in MSI, for example DESI (Wu et al., 2009). A chemical reaction appropriate for on-tissue derivatization in MALDI-MSI experiments should be efficient and rapid, so as to avoid delocalization of chemicals on the tissue section from their original location (Goodwin, 2012). The reactive DESI paper where betaine aldehyde is used suggest a rapid derivatization of cholesterol,

indicating that this reaction is applicable in MALDI-MSI as well. The BA derivatized cholesterol forms a peak at 488.4 and is easily ionized due to the inherent charge. The derivatization preparation yielded a signal in the 50-100 a.u., which is a signal intensity increase in the range of 10-20 fold compared with non-derivatized cholesterol, whether or not the washing step had been employed, lending support to the use of this successful derivatization step in the final method.

The distribution of the cholesterol derivative was in some instances not like what was witnessed before in this project. In Figure 17 where slide S06 was analyzed the distribution of the derivatized cholesterol on the control tissue does not follow the areas of major lipid structures but this could be a flaw in this particular control section as the sham lesioned tissue section on the same slide exhibits the normal distribution pattern noticed in earlier runs.

The other disparity noticed in the distribution is that in Figures 17 and 18, containing slides S06 and S07 respectively, a significant signal appears off-tissue. This off-tissue signal could be due to delocalization of the derivatized cholesterol when the BA reactant is applied, as the BA-cholesterol-derivative is estimated to be soluble in aqueous solutions. In an effort to decrease this analyte delocalization, another method for applying the BA reactant was tested; the ImagePrep automated sprayer (Figure 19, containing slide S08). Here, since a higher concentration of BA was tested, an increased overall signal of the derivative is noticed and, possibly because of a gentler spray method compared to the TLC sprayer, less signal is visualized off-tissue. A tandem MS spectra was collected of the derivatized parent ion (488) after MALDI-MSI analysis of slide S08 and the fragments associated with cholesterol and two fragments belonging to BA (m/z 102 & 120) are depicted in Figure 20. Importantly, it was now possible to visualize the spatial distribution of the fragmented ion on tissue. In conclusion, the identification of the derivitized cholesterol was achieved. The only thing that could be improved when inspecting slide S08 in Figure 19 is a higher distribution in the aforementioned lipid rich structures. This motivated the interest in combining the two preparation steps into one method, where the tissue is washed prior to the derivatization sample preparation. This curiosity prompted the preparation of slide S09 (Figures 21, 22 and 23) where, like before in the washing preparation development, one half containing one control and one sham lesioned brain section is washed and the direct comparison of

consecutive tissue sections was performed. The results from this MALDI-MSI run are conclusive of the benefit of utilizing the washing preparation prior to derivatizing cholesterol. Visually, the relative abundance of the derivative peak on the washed tissues is so high that the unwashed tissue sections seem to contain hardly any derivatized cholesterol at all in comparison. The distribution of the signal is also in a manner to be expected, that is higher relative abundance in the corpus callosum and the striatum while still containing high signal in the entire brain tissue section (Dietschy & Turley, 2004; Trim et al., 2008; Veloso et al., 2011). There is still some signal found in the off-tissue area, which could point to it being beneficial to use less of the BA reactant or to alter the ImagePrep dispersion application is some way. This combined method increased the overall average signal of the analyte by a factor of 3.4 and moved the signal from around the 50-150 a.u. region up to well above the 400 a.u. region. It is of interest to note that while the washing preparation with 100 mM buffer concentration increased the cholesterol signal twofold, the same washing preparation increased the signal intensity of the derivatized cholesterol product by up to fourfold. This difference can be speculated to arise from better penetration of the reactant with increased accessibility to the cholesterol deposits once other chemicals such as salts and other water-soluble substances have been removed.

The comparison of using the new developed sample preparation method is shown in Figure 24, where the signal intensity of cholesterol and the cholesterol derivative on control tissues from slides S02 and S08 are compared. Slide S02 did not utilize the washing and derivatization sample preparation method developed unlike slide S08 and the difference is clear. The signal intensity of cholesterol in the control tissue from slide S02 is 3.2 a.u. compared with 472 a.u. on slide S08. So the sample preparation method increased the signal intensity by a factor of 148.

5.2 Implementation of the newly developed method to visualize cholesterol in a PD-model

Since the sample preparation method developed to visualize the MALDI-MSI relative abundance and distribution of cholesterol seemed powerful enough it was implemented in the examination of cholesterol within the brain section of a rat model of PD. The PD-

model brain sections were added to two slides also containing a control section and a sham lesioned section, slides S10 and S11 (Figures 17 and 18). The MALDI-MSI results from these two slides show the strength of the new sample preparation method as both slides (S10 and S11) are comparable in the relative abundance of the derivative peak (m/z 488) and the distribution of the derivative across the tissue section. The only difference between the two slides is that slide S11 (figure 18) was reacted with a lower concentration of BA, 63 μg/mL compared with 126 μg/mL in slide S10 and slide S09.

The object of this experiment was to see if a difference in abundance of cholesterol could be detected between the hemispheres in a rat model of PD brain tissue. Both Figures 17 and 18 containing slides S10 and S11 have no apparent difference in the distribution of the cholesterol derivative, which can be considered a substitute of cholesterol, between the PD lesioned and unlesioned hemispheres. Thus, these preliminary data suggest that there is no difference in the abundance of cholesterol between the lesioned and unlesioned hemisphere of PD model rats.

Care must be taken not jump to conclusions in translating these results directly to PD. The toxin induced PD rat model these results are based on only partially mimics the disease by depleting the DA stores of certain areas of the hemisphere it is injected to, and is thus often referred to a hemiparkinsons model (Schober, 2004). This toxin does not replicate the progressive loss of dopaminergic neurons or cause the pathogenic hallmark of PD, the LB containing the protein α-synuclein (Schober, 2004), meaning α-synuclein is not a part of the pathogenic route of the toxin (Schober, 2004). As interplay has been noticed between cholesterol in the brain and the protein α-synuclein, where for instance cholesterol has been observed in α-synuclein aggregations, this mechanism connecting cholesterol levels with PD could go unnoticed in the 6-OHDA hemiparkinson model (Liu et al., 2010; Schober, 2004). Another factor that must be assessed is that this project only analyzed two consecutive sections from the same PD model rat. Further experiments analyzing the abundance and distribution of cholesterol in a suitable PD model would be needed to make an accurate assessment of the connection between cholesterol in the brain and Parkinson's disease.

5.3 Strengths and limitations

The development of a sample preparation method led to the comparison of cholesterol levels between healthy and PD-model tissue using a tool, the MALDI-MSI, especially qualified for this kind of comparison (Ye et al., 2012). The use of a fully automated matrix sprayer, the TM sprayer, to matrix coat the samples generates a homogenous matrix layer for consistent results and the other automated sprayer used, the ImagePrep, was utilized for dispersion of the reactant in the derivatization step. The use of these automated sprayers is beneficial if minor tweaking of the sample preparation method is needed as simple settings on the machines can be adjusted for this.

Previous studies conclude DHB to be the most appropriate matrix for the inspection of cholesterol (Jackson, Wang, & Woods, 2005; McAvey, Guan, Fortier, Tarr, & Cole, 2011). However, since the derivatization step was previously used in a DESI-MSI paper where no matrix is used (Wu et al., 2009), it could have been informative to test other matrices as well. More optimization of the method via tweaking of the BA concentration and trying different concentrations of the buffer, perhaps a concentration in between the two tested in this project would also have been informative.

5.4 Future perspectives

This sample preparation method could be used to test additional brain tissues from different rats and perhaps change the PD-model from the toxin induced model to a model more applicable with the disease, possibly a genetic PD animal model showing the pathogenic hallmarks of PD with α-synuclein and LB (Schober, 2004). Added interest could be to quantify the amount of cholesterol directly on the brain tissue. This could be performed by adding a quantification step within the described sample preparation method. A recent paper presented a software capable of doing absolute quantification, instead of the relative abundance, using a deuterated form of the analyte to aid quantitation (Källback et al., 2012). As the isotope labeled form of cholesterol has already been used in the derivatized article (Wu et al., 2009), this could be possible.

This sample preparation method could be utilized to analyze substances of the same chemical nature as cholesterol. These describe molecules that contain a large carbohydrate build with a single hydroxyl group. As these molecules are expected not to be soluble in water, the washing preparation step would not remove them from tissue being inspected and the BA derivatization is especially useful for molecules similar to cholesterol (Wu et al., 2009). The molecules this could be applicable to a number of high interest molecules such as fat-soluble vitamins for instance vitamin D and A, and theoretically this preparation method could aid the detection of certain neurosteroids which have received a lot of interest lately because of their involvement in a number of brain processes (Zorumski, Paul, Izumi, Covey, & Mennerick, 2013).

6. CONCLUSIONS

The sample preparation method developed in this project was successful in increasing the signal intensity and allowing for an enhanced visualization of the relative abundance and distribution of cholesterol within a rat brain tissue utilizing MALDI-MSI as well as enabling on-tissue identification of cholesterol via MS/MS. The results demonstrate that a combination of a washing preparation step and a derivatization step dramatically increased the signal intensity compared with no sample preparation.

When implemented in a PD-model the results showed no difference in cholesterol's relative abundance between the neurotoxin-lesioned (dopamine depleted) hemisphere and the healthy tissue. These preliminary data suggest that cholesterol levels are not affected in a neurotoxin induced rat model of PD, however the overall quality of this particular PD-model should be assessed before any conclusions can be finalized. In addition, further research is needed to evaluate the proposed association between the cholesterol abundance and PD.

In extension, the described sample preparation method is applicable for the analysis of other similar molecules to cholesterol. These include certain interesting molecules such as vitamin D, vitamin A, neurosteroids and other molecules with similar structures.

7. ACKNOWLEDGEMENTS

The work presented in this thesis was carried out at the Medical Mass Spectrometry Unit at the Department of Pharmaceutical Biosciences at Uppsala University. I am very thankful for the great opportunity of doing my thesis in this thriving research environment with a knowledgeable group.

I want to thank my supervisor Margrét Þorsteinsdóttir and my two instructors Cecilia Eriksson and Per Andrén for all their guidance and support during the project. You have given me opportunities to develop my research capacities, given me good advises and shared your wealth of knowledge with me. I would also like to thank Mohammadreza Shariatgorji for all his guidance and patience during the work on this project.

I would like to thank all the employees at the unit of Medical Mass Spectrometry for their support and fellowship. Also I would like to thank my teachers and fellow students at the Faculty of Pharmaceutical Sciences at the University of Iceland. Finally I would like to thank my loving girlfriend Birna Þórisdóttir for all her support and help during the work on the thesis as well as my family for their support throughout my education.

8. REFERENCES

Alberio, T., & Fasano, M. (2011). Proteomics in Parkinson's disease: An unbiased approach towards peripheral biomarkers and new therapies. *Journal of Biotechnology, 156*(4), 325-337. doi: 10.1016/j.jbiotec.2011.08.004

Anchisi, L., Dessi, S., Pani, A., & Mandas, A. (2012). Cholesterol homeostasis: a key to prevent or slow down neurodegeneration. *Front Physiol, 3*, 486. doi: 10.3389/fphys.2012.00486

Angel, P. M., Spraggins, J. M., Baldwin, H. S., & Caprioli, R. (2012). Enhanced Sensitivity for High Spatial Resolution Lipid Analysis by Negative Ion Mode MALDI Imaging Mass Spectrometry. *Analytical Chemistry, 84*(3), 1557-1564. doi: 10.1021/ac202383m

Aqul, A., Liu, B., Ramirez, C. M., Pieper, A. A., Estill, S. J., Burns, D. K., . . . Dietschy, J. M. (2011). Unesterified Cholesterol Accumulation in Late Endosomes/Lysosomes Causes Neurodegeneration and Is Prevented by Driving Cholesterol Export from This Compartment. *The Journal of Neuroscience, 31*(25), 9404-9413. doi: 10.1523/jneurosci.1317-11.2011

Bar-On, P., Crews, L., Koob, A. O., Mizuno, H., Adame, A., Spencer, B., & Masliah, E. (2008). Statins reduce neuronal α-synuclein aggregation in in vitro models of Parkinson's disease. *Journal of Neurochemistry, 105*(5), 1656-1667. doi: 10.1111/j.1471-4159.2008.05254.x

Barceló-Coblijn, G., Golovko, M. Y., Weinhofer, I., Berger, J., & Murphy, E. J. (2007). Brain neutral lipids mass is increased in α-synuclein gene-ablated mice. *Journal of Neurochemistry, 101*(1), 132-141. doi: 10.1111/j.1471-4159.2006.04348.x

Björkhem, I., Lütjohann, D., Diczfalusy, U., Ståhle, L., Ahlborg, G., & Wahren, J. (1998). Cholesterol homeostasis in human brain: turnover of 24S-hydroxycholesterol and evidence for a cerebral origin of most of this oxysterol in the circulation. *Journal of Lipid Research, 39*(8), 1594-1600.

Bosco, D. A., Fowler, D. M., Zhang, Q., Nieva, J., Powers, E. T., Wentworth, P., . . . Kelly, J. W. (2006). Elevated levels of oxidized cholesterol metabolites in Lewy body disease brains accelerate α-synuclein fibrilization. *Nature Chemical Biology, 2*(5), 249-253. doi: 10.1038/nchembio782

Brooks, D. J. (2012). Parkinson's disease: Diagnosis. *Parkinsonism & Related Disorders, 18, Supplement 1*(0), S31-S33. doi: http://dx.doi.org/10.1016/S1353-8020(11)70012-8

Cameron, L. C. (2012). Mass spectrometry imaging: Facts and perspectives from a non-mass spectrometrist point of view. *Methods, 57*(4), 417-422. doi: 10.1016/j.ymeth.2012.06.007

Caprioli, R. M., Farmer, T. B., & Gile, J. (1997). Molecular Imaging of Biological Samples: Localization of Peptides and Proteins Using MALDI-TOF MS. *Analytical Chemistry, 69*(23), 4751-4760. doi: 10.1021/ac970888i

Chang, T. Y., Chang, C. C., Ohgami, N., & Yamauchi, Y. (2006). Cholesterol sensing, trafficking, and esterification. *Annu Rev Cell Dev Biol, 22*, 129-157. doi: 10.1146/annurev.cellbio.22.010305.104656

Chaurand, P. (2012). Imaging mass spectrometry of thin tissue sections: A decade of collective efforts. *Journal of Proteomics, 75*(16), 4883-4892. doi: 10.1016/j.jprot.2012.04.005

Davis, R. A., Sinensky, M., & Junker, L. H. (1989). Regulation of cholesterol synthesis and the potential for its pharmacologic manipulation. *Pharmacology & Therapeutics, 43*(2), 221-236. doi: http://dx.doi.org/10.1016/0163-7258(89)90119-8

Deininger, S.-O., Cornett, D., Paape, R., Becker, M., Pineau, C., Rauser, S., . . . Wolski, E. (2011). Normalization in MALDI-TOF imaging datasets of proteins: practical considerations. *Analytical and Bioanalytical Chemistry, 401*(1), 167-181. doi: 10.1007/s00216-011-4929-z

Denson, M. A., & Wszolek, Z. K. (1995). Familial parkinsonism: Our experience and review. *Parkinsonism & Related Disorders, 1*(1), 35-46. doi: http://dx.doi.org/10.1016/1353-8020(95)00010-4

Dietschy, J. M. (2009). Central nervous system: cholesterol turnover, brain development and neurodegeneration. *Biological chemistry, 390*(4), 287-293. doi: 10.1515/bc.2009.035

Dietschy, J. M., & Turley, S. D. (2004). Thematic review series: Brain Lipids. Cholesterol metabolism in the central nervous system during early development

and in the mature animal. *Journal of Lipid Research, 45*(8), 1375-1397. doi: 10.1194/jlr.R400004-JLR200

Duncan, M. W., Roder, H., & Hunsucker, S. W. (2008). Quantitative matrix-assisted laser desorption/ionization mass spectrometry. *Briefings in Functional Genomics and Proteomics, 7*(5), 355-370. doi: 10.1093/bfgp/eln041

Fortin, D. L., Troyer, M. D., Nakamura, K., Kubo, S.-i., Anthony, M. D., & Edwards, R. H. (2004). Lipid Rafts Mediate the Synaptic Localization of α-Synuclein. *The Journal of Neuroscience, 24*(30), 6715-6723. doi: 10.1523/jneurosci.1594-04.2004

Fuchs, B., Süß, R., & Schiller, J. (2010). An update of MALDI-TOF mass spectrometry in lipid research. *Progress in Lipid Research, 49*(4), 450-475. doi: 10.1016/j.plipres.2010.07.001

Gamba, P., Testa, G., Sottero, B., Gargiulo, S., Poli, G., & Leonarduzzi, G. (2012). The link between altered cholesterol metabolism and Alzheimer's disease. *Ann N Y Acad Sci, 1259*, 54-64. doi: 10.1111/j.1749-6632.2012.06513.x

Goodwin, R. J. A. (2012). Sample preparation for mass spectrometry imaging: Small mistakes can lead to big consequences. *Journal of Proteomics, 75*(16), 4893-4911. doi: 10.1016/j.jprot.2012.04.012

Goto-Inoue, N., Hayasaka, T., Zaima, N., & Setou, M. (2011). Imaging mass spectrometry for lipidomics. *Biochimica et Biophysica Acta (BBA) - Molecular and Cell Biology of Lipids, 1811*(11), 961-969. doi: 10.1016/j.bbalip.2011.03.004

Grünblatt, E. (2012). Parkinson's disease: Molecular risk factors. *Parkinsonism & Related Disorders, 18, Supplement 1*(0), S45-S48. doi: http://dx.doi.org/10.1016/S1353-8020(11)70016-5

Haas, B. R., Stewart, T. H., & Zhang, J. (2012). Premotor biomarkers for Parkinson's disease - a promising direction of research. *Transl Neurodegener, 1*(1), 11. doi: 10.1186/2047-9158-1-11

Hayashi, H. (2011). Lipid Metabolism and Glial Lipoproteins in the Central Nervous System. *Biological and Pharmaceutical Bulletin, 34*(4), 453-461.

Hayashi, H., Campenot, R. B., Vance, D. E., & Vance, J. E. (2004). Glial Lipoproteins Stimulate Axon Growth of Central Nervous System Neurons in Compartmented

Cultures. *Journal of Biological Chemistry, 279*(14), 14009-14015. doi: 10.1074/jbc.M313828200

Heeren, R. M. A., Smith, D. F., Stauber, J., Kükrer-Kaletas, B., & MacAleese, L. (2009). Imaging Mass Spectrometry: Hype or Hope? *Journal of The American Society for Mass Spectrometry, 20*(6), 1006-1014. doi: 10.1016/j.jasms.2009.01.011

Hindle, J. V. (2010). Ageing, neurodegeneration and Parkinson's disease. *Age Ageing, 39*(2), 156-161. doi: 10.1093/ageing/afp223

Ikonen, E. (2008). Cellular cholesterol trafficking and compartmentalization. *Nat Rev Mol Cell Biol, 9*(2), 125-138. doi: 10.1038/nrm2336

Jackson, S. N., Wang, H.-Y. J., & Woods, A. S. (2005). Direct Profiling of Lipid Distribution in Brain Tissue Using MALDI-TOFMS. *Analytical Chemistry, 77*(14), 4523-4527. doi: 10.1021/ac050276v

Jankovic, J. (2008). Parkinson's disease: clinical features and diagnosis. *J Neurol Neurosurg Psychiatry, 79*(4), 368-376. doi: 10.1136/jnnp.2007.131045

Johnson, D. W., Brink, H. J. t., & Jakobs, C. (2001). A rapid screening procedure for cholesterol and dehydrocholesterol by electrospray ionization tandem mass spectrometry. *Journal of Lipid Research, 42*(10), 1699-1705.

Jungmann, J. H., & Heeren, R. M. A. (2012). Emerging technologies in mass spectrometry imaging. *Journal of Proteomics, 75*(16), 5077-5092. doi: 10.1016/j.jprot.2012.03.022

Källback, P., Shariatgorji, M., Nilsson, A., & Andrén, P. E. (2012). Novel mass spectrometry imaging software assisting labeled normalization and quantitation of drugs and neuropeptides directly in tissue sections. *Journal of Proteomics, 75*(16), 4941-4951. doi: http://dx.doi.org/10.1016/j.jprot.2012.07.034

Kamp, F., & Beyer, K. (2006). Binding of α-Synuclein Affects the Lipid Packing in Bilayers of Small Vesicles. *Journal of Biological Chemistry, 281*(14), 9251-9259. doi: 10.1074/jbc.M512292200

Li, Y., Shrestha, B., & Vertes, A. (2006). Atmospheric Pressure Molecular Imaging by Infrared MALDI Mass Spectrometry. *Analytical Chemistry, 79*(2), 523-532. doi: 10.1021/ac061577n

Li, Y., Shrestha, B., & Vertes, A. (2007). Atmospheric Pressure Infrared MALDI Imaging Mass Spectrometry for Plant Metabolomics. *Analytical Chemistry, 80*(2), 407-420. doi: 10.1021/ac701703f

Licker, V., Kövari, E., Hochstrasser, D. F., & Burkhard, P. R. (2009). Proteomics in human Parkinson's disease research. *Journal of Proteomics, 73*(1), 10-29. doi: 10.1016/j.jprot.2009.07.007

Liebisch, G., Binder, M., Schifferer, R., Langmann, T., Schulz, B., & Schmitz, G. (2006). High throughput quantification of cholesterol and cholesteryl ester by electrospray ionization tandem mass spectrometry (ESI-MS/MS). *Biochimica et Biophysica Acta (BBA) - Molecular and Cell Biology of Lipids, 1761*(1), 121-128. doi: 10.1016/j.bbalip.2005.12.007

Liu, J. P., Tang, Y., Zhou, S., Toh, B. H., McLean, C., & Li, H. (2010). Cholesterol involvement in the pathogenesis of neurodegenerative diseases. *Mol Cell Neurosci, 43*(1), 33-42. doi: 10.1016/j.mcn.2009.07.013

Lund, E. G., Guileyardo, J. M., & Russell, D. W. (1999). cDNA cloning of cholesterol 24-hydroxylase, a mediator of cholesterol homeostasis in the brain. *Proceedings of the National Academy of Sciences of the United States of America, 96*(13), 7238-7243.

Lutjohann, D., Breuer, O., Ahlborg, G., Nennesmo, I., Siden, A., Diczfalusy, U., & Bjorkhem, I. (1996). Cholesterol homeostasis in human brain: evidence for an age-dependent flux of 24S-hydroxycholesterol from the brain into the circulation. *Proceedings of the National Academy of Sciences of the United States of America, 93*(18), 9799-9804.

Mahley, R. W., Weisgraber, K. H., & Huang, Y. (2006). Apolipoprotein E4: A causative factor and therapeutic target in neuropathology, including Alzheimer's disease. *Proceedings of the National Academy of Sciences, 103*(15), 5644-5651. doi: 10.1073/pnas.0600549103

Mauch, D. H., Nägler, K., Schumacher, S., Göritz, C., Müller, E.-C., Otto, A., & Pfrieger, F. W. (2001). CNS Synaptogenesis Promoted by Glia-Derived Cholesterol. *Science, 294*(5545), 1354-1357. doi: 10.1126/science.294.5545.1354

McAvey, K. M., Guan, B., Fortier, C. A., Tarr, M. A., & Cole, R. B. (2011). Laser-Induced Oxidation of Cholesterol Observed During MALDI-TOF Mass Spectrometry. *Journal of The American Society for Mass Spectrometry, 22*(4), 659-669. doi: 10.1007/s13361-011-0074-3

Minovici, S., & Vanghelovici, M. (1934). Contributions to our knowledge of cholesterol. *Journal of Chemical Education, 11*(12). doi: 10.1021/ed011p637

Muller, T. (2012). Drug therapy in patients with Parkinson's disease. *Transl Neurodegener, 1*(1), 10. doi: 10.1186/2047-9158-1-10

Murphy, R. C., Hankin, J. A., & Barkley, R. M. (2008). Imaging of lipid species by MALDI mass spectrometry. *The Journal of Lipid Research, 50*(Supplement), S317-S322. doi: 10.1194/jlr.R800051-JLR200

Nieweg, K., Schaller, H., & Pfrieger, F. W. (2009). Marked differences in cholesterol synthesis between neurons and glial cells from postnatal rats. *Journal of Neurochemistry, 109*(1), 125-134. doi: 10.1111/j.1471-4159.2009.05917.x

Ozansoy, M., & Basak, A. N. (2012). The Central Theme of Parkinson's Disease: alpha-Synuclein. *Mol Neurobiol*. doi: 10.1007/s12035-012-8369-3

Piehowski, P. D., Carado, A. J., Kurczy, M. E., Ostrowski, S. G., Heien, M. L., Winograd, N., & Ewing, A. G. (2008). MS/MS Methodology To Improve Subcellular Mapping of Cholesterol Using TOF-SIMS. *Analytical Chemistry, 80*(22), 8662-8667. doi: 10.1021/ac801591r

Rantham Prabhakara, J. P., Feist, G., Thomasson, S., Thompson, A., Schommer, E., & Ghribi, O. (2008). Differential effects of 24-hydroxycholesterol and 27-hydroxycholesterol on tyrosine hydroxylase and α-synuclein in human neuroblastoma SH-SY5Y cells. *Journal of Neurochemistry, 107*(6), 1722-1729. doi: 10.1111/j.1471-4159.2008.05736.x

Samii, A., Nutt, J. G., & Ransom, B. R. (2004). Parkinson's disease. *The Lancet, 363*(9423), 1783-1793. doi: http://dx.doi.org/10.1016/S0140-6736(04)16305-8

Sandhoff, R., Brügger, B., Jeckel, D., Lehmann, W. D., & Wieland, F. T. (1999). Determination of cholesterol at the low picomole level by nano-electrospray ionization tandem mass spectrometry. *Journal of Lipid Research, 40*(1), 126-132.

Schiller, J., Süß, R., Arnhold, J., Fuchs, B., Leßig, J., Müller, M., . . . Arnold, K. (2004). Matrix-assisted laser desorption and ionization time-of-flight (MALDI-TOF) mass spectrometry in lipid and phospholipid research. *Progress in Lipid Research, 43*(5), 449-488. doi: 10.1016/j.plipres.2004.08.001

Schober, A. (2004). Classic toxin-induced animal models of Parkinson's disease: 6-OHDA and MPTP. *Cell and Tissue Research, 318*(1), 215-224. doi: 10.1007/s00441-004-0938-y

Schwamborn, K. (2012). Imaging mass spectrometry in biomarker discovery and validation. *Journal of Proteomics, 75*(16), 4990-4998. doi: 10.1016/j.jprot.2012.06.015

Schwamborn, K., & Caprioli, R. M. (2010). MALDI Imaging Mass Spectrometry – Painting Molecular Pictures. *Molecular Oncology, 4*(6), 529-538. doi: 10.1016/j.molonc.2010.09.002

Shariatgorji, M., Källback, P., Gustavsson, L., Schintu, N., Svenningsson, P., Goodwin, R. J. A., & Andren, P. E. (2012). Controlled-pH Tissue Cleanup Protocol for Signal Enhancement of Small Molecule Drugs Analyzed by MALDI-MS Imaging. *Analytical Chemistry, 84*(10), 4603-4607. doi: 10.1021/ac203322q

Simons, K., & Ehehalt, R. (2002). Cholesterol, lipid rafts, and disease. *Journal of Clinical Investigation, 110*(5), 597-603. doi: 10.1172/jci16390

Steck, T. L., & Lange, Y. (2010). Cell cholesterol homeostasis: Mediation by active cholesterol. *Trends in cell biology, 20*(11), 680-687.

Suckau, D., Resemann, A., Schuerenberg, M., Hufnagel, P., Franzen, J., & Holle, A. (2003). A novel MALDI LIFT-TOF/TOF mass spectrometer for proteomics. *Analytical and Bioanalytical Chemistry, 376*(7), 952-965. doi: 10.1007/s00216-003-2057-0

Tabas, I. (2002). Consequences of cellular cholesterol accumulation: basic concepts and physiological implications. *Journal of Clinical Investigation, 110*(7), 905-911. doi: 10.1172/jci0216452

Thomas, B., & Beal, M. F. (2007). Parkinson's disease. *Hum Mol Genet, 16 Spec No. 2*, R183-194. doi: 10.1093/hmg/ddm159

Thomas, B., & Beal, M. F. (2011). Molecular insights into Parkinson's disease. *F1000 Med Rep, 3*, 7. doi: 10.3410/m3-7

Tian, Q., Failla, M. L., Bohn, T., & Schwartz, S. J. (2006). High-performance liquid chromatography/atmospheric pressure chemical ionization tandem mass spectrometry determination of cholesterol uptake by Caco-2 cells. *Rapid Communications in Mass Spectrometry, 20*(20), 3056-3060. doi: 10.1002/rcm.2700

Touboul, D., Brunelle, A., & Laprévote, O. (2011). Mass spectrometry imaging: Towards a lipid microscope? *Biochimie, 93*(1), 113-119. doi: 10.1016/j.biochi.2010.05.013

Trim, P. J., Atkinson, S. J., Princivalle, A. P., Marshall, P. S., West, A., & Clench, M. R. (2008). Matrix-assisted laser desorption/ionisation mass spectrometry imaging of lipids in rat brain tissue with integrated unsupervised and supervised multivariant statistical analysis. *Rapid Communications in Mass Spectrometry, 22*(10), 1503-1509. doi: 10.1002/rcm.3498

Valente, E. M., Arena, G., Torosantucci, L., & Gelmetti, V. (2012). Molecular pathways in sporadic PD. *Parkinsonism & Related Disorders, 18, Supplement 1*(0), S71-S73. doi: http://dx.doi.org/10.1016/S1353-8020(11)70023-2

Veloso, A., Fernández, R., Astigarraga, E., Barreda-Gómez, G., Manuel, I., Giralt, M. T., . . . Fernández, J. (2011). Distribution of lipids in human brain. *Analytical and Bioanalytical Chemistry, 401*(1), 89-101. doi: 10.1007/s00216-011-4882-x

Wu, C., Ifa, D. R., Manicke, N. E., & Cooks, R. G. (2009). Rapid, Direct Analysis of Cholesterol by Charge Labeling in Reactive Desorption Electrospray Ionization. *Analytical Chemistry, 81*(18), 7618-7624. doi: 10.1021/ac901003u

Xie, C., Lund, E. G., Turley, S. D., Russell, D. W., & Dietschy, J. M. (2003). Quantitation of two pathways for cholesterol excretion from the brain in normal mice and mice with neurodegeneration. *Journal of Lipid Research, 44*(9), 1780-1789. doi: 10.1194/jlr.M300164-JLR200

Ye, H., Gemperline, E., & Li, L. (2012). A vision for better health: Mass spectrometry imaging for clinical diagnostics. *Clinica Chimica Acta*. doi: 10.1016/j.cca.2012.10.018

Zhang, X., Andren, P. E., Greengard, P., & Svenningsson, P. (2008). Evidence for a role of the 5-HT1B receptor and its adaptor protein, p11, in l-DOPA treatment of an

animal model of Parkinsonism. *Proceedings of the National Academy of Sciences, 105*(6), 2163-2168. doi: 10.1073/pnas.0711839105

Zorumski, C. F., Paul, S. M., Izumi, Y., Covey, D. F., & Mennerick, S. (2013). Neurosteroids, stress and depression: Potential therapeutic opportunities. *Neuroscience & Biobehavioral Reviews, 37*(1), 109-122. doi: 10.1016/j.neubiorev.2012.10.005

9. APPENDIX

Appendix I: Additional MALDI-MSI results without sample preparation method

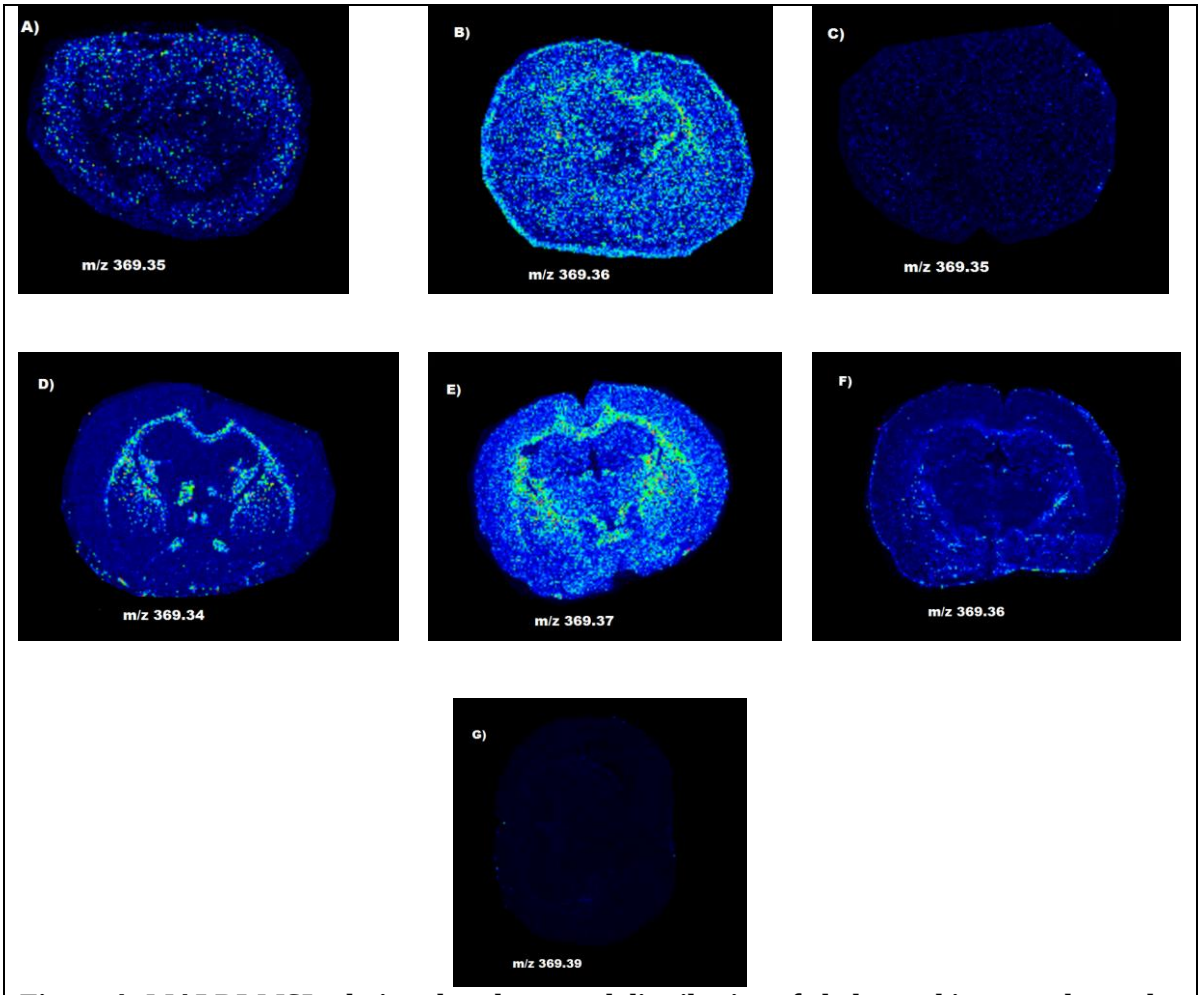

Figure A. MALDI-MSI relative abundance and distribution of cholesterol in control samples from additional runs where the sample preparation method was not used. Images use different matrix solvents with different concentrations of the DHB matrix, the TLC-sprayer was used for matrix application. Images were collected with 100µm spatial resolution.. The different analysis were performed in the order depicted A)-I). A) 20mg/mL DHB in 50% EtOH. B) 20mg/mL DHB in 50% EtOH.. C) 50mg/mL DHB in 80% EtOH with 0.1% TFA. D) 50mg/mL DHB in chloroform/MetOH/H2O (65/25/4) with 0.2% TFA. E) 50mg/mL DHB in chloroform/MetOH/H2O (65/25/4) with 0.2% TFA. F) 50mg/mL DHB in 50% ACN with 0.2% TFA.. G) 50mg/mL DHB in 50% ACN with 0.2% TFA. Images were TIC normalized

Figure A shows additional MALDI-MSI results from runs where a sample preparation method was not used. Images F) and G) in Figure A used the same method as Image B) in Figure 8 (4.1.1 MALDI-MSI without sample preparation method).

Appendix II: Additional MALDI-MSI results without sample preparation method

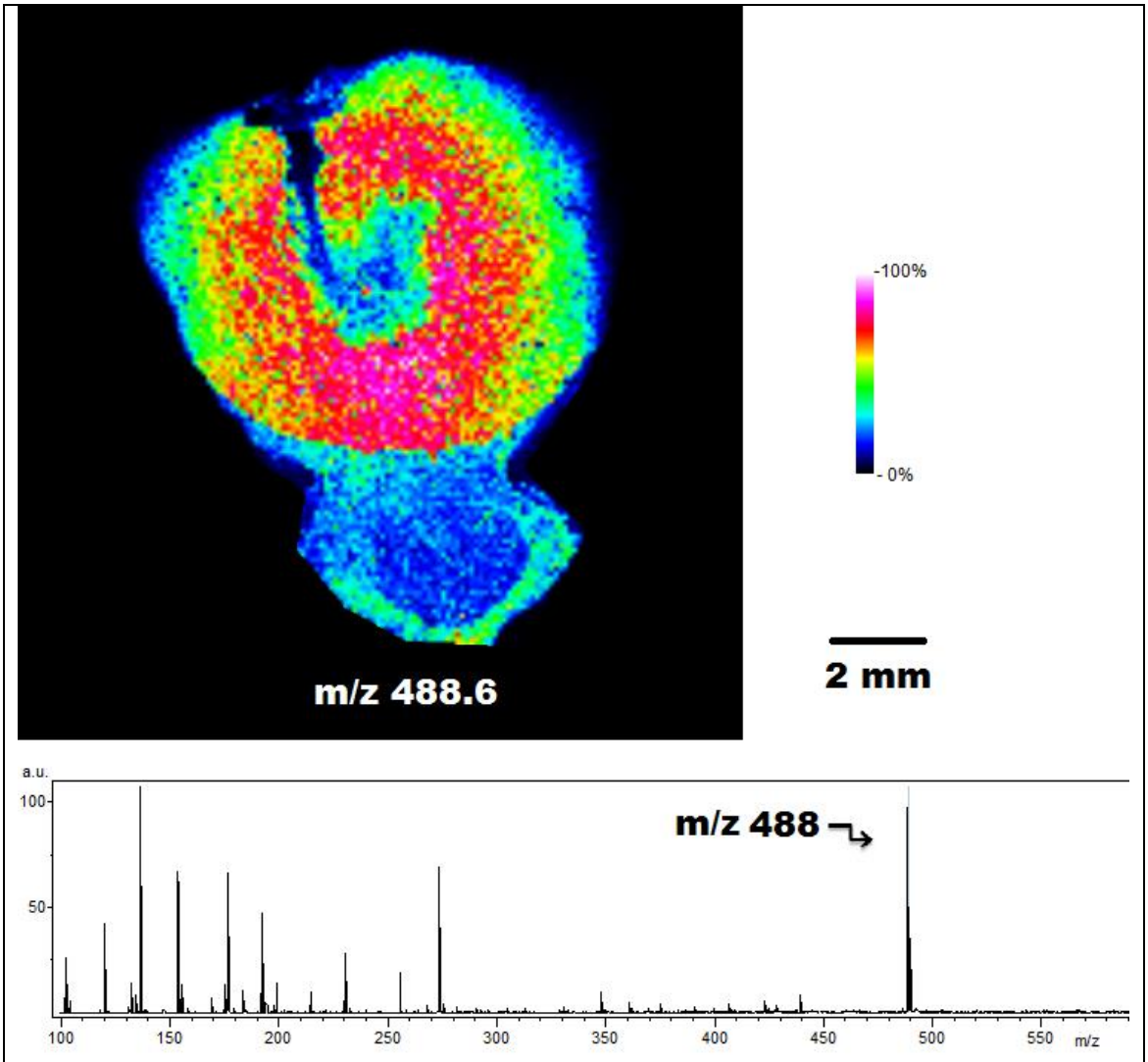

Figure B. MALDI-MSI results from the first test of BA derivatization using a dropper for the application of the BA solution directly on half of control sample. The derivative peak (m/z 488) is shown.

Figure B depicts the first testing of the derivatization method (see 4.1.3 MALDI-MSI using derivatization method) using a dropper to directly apply the reactant to half of a control tissue sample.